Aerothermal and Propulsion Ground Testing That Can Be Conducted to Increase Chances for Successful Hypervelocity Flight Experiments

Michael S. Holden, PhD
CUBRC
4455 Genesee Street
Buffalo, NY 14225 USA
holden@cubrc.org

1.0 OUTLINE

- Introduction – Experiment/Testing in Flight and on Ground
- Requirements for Ground Test Simulation in Hypersonic/Hypervelocity Flows
- Mach Number/Reynolds Number Simulation and Aerothermal Tests for Shuttle
- Numerical Codes/Physical Models Evaluation Studies
- Velocity/Density Simulation and Evaluation of Vehicle Performance
- Velocity/Altitude Simulation and Scramjet Engine Testing
- Conclusions

2.0 INTRODUCTION – EXPERIMENT/TESTING IN FLIGHT AND ON THE GROUND

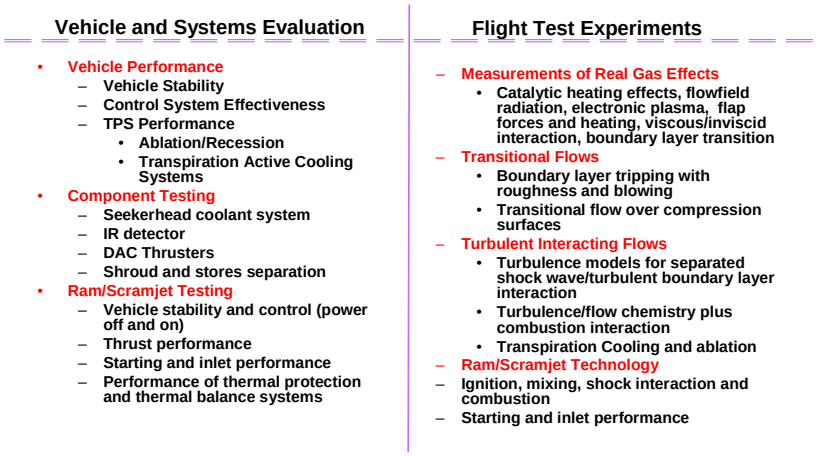

Figure 1: Flight Tests and Flight Experiments

In general there are two types of flight tests. As illustrated in Figure 1, the first type is to evaluate vehicle performance and systems, and the second type of flight tests is to perform experiments to evaluate key phenomena, the results of which would be employed to validate prediction techniques and improve models of physical phenomena employed in the numerical codes. Vehicle stability and control are of major concern in the vehicle flight tests, as well as TPS performance, and the performance of control thrusters and other guidance components. In tests of Ram or Scramjets, evaluating vehicle thrust is of primary importance followed by the performance of thermal protection systems. The major areas of interest in flight tests experiments are real gas effects, boundary layer

Holden, M.S. (2007) Aerothermal and Propulsion Ground Testing That Can Be Conducted to Increase Chances for Successful Hypervelocity Flight Experiments. In *Flight Experiments for Hypersonic Vehicle Development* (pp. 1-1 – 1-36). Educational Notes RTO-EN-AVT-130, Paper 1. Neuilly-sur-Seine, France: RTO. Available from: http://www.rto.nato.int/abstracts.asp.

Report Documentation Page

Form Approved
OMB No. 0704-0188

1. REPORT DATE	2. REPORT TYPE	3. DATES COVERED
01 JUN 2007	**N/A**	**-**

4. TITLE AND SUBTITLE	5a. CONTRACT NUMBER
Aerothermal and Propulsion Ground Testing That Can Be Conducted to Increase Chances for Successful Hypervelocity Flight Experiments	5b. GRANT NUMBER
	5c. PROGRAM ELEMENT NUMBER
6. AUTHOR(S)	5d. PROJECT NUMBER
	5e. TASK NUMBER
	5f. WORK UNIT NUMBER
7. PERFORMING ORGANIZATION NAME(S) AND ADDRESS(ES) **CUBRC 4455 Genesee Street Buffalo, NY 14225 USA**	8. PERFORMING ORGANIZATION REPORT NUMBER
9. SPONSORING/MONITORING AGENCY NAME(S) AND ADDRESS(ES)	10. SPONSOR/MONITOR'S ACRONYM(S)
	11. SPONSOR/MONITOR'S REPORT NUMBER(S)

12. DISTRIBUTION/AVAILABILITY STATEMENT
Approved for public release, distribution unlimited

13. SUPPLEMENTARY NOTES
See also ADM002054., The original document contains color images.

14. ABSTRACT

15. SUBJECT TERMS

16. SECURITY CLASSIFICATION OF:			17. LIMITATION OF ABSTRACT	18. NUMBER OF PAGES	19a. NAME OF RESPONSIBLE PERSON
a. REPORT	b. ABSTRACT	c. THIS PAGE			
unclassified	**unclassified**	**unclassified**	**UU**	**36**	

Standard Form 298 (Rev. 8-98)
Prescribed by ANSI Std Z39-18

transition, viscous interaction phenomena in laminar and turbulent flows, and ignition, mixing, shock interaction and combustion phenomena for airbreathing systems.

- Real gas effects on laminar interacting flows
  - Computational methods to describe flows between rarified and continuum flow regimes
  - Models of real gas chemistry for velocities above 10,000 ft/s
  - Models of flow/surface interaction in hypervelocity flows
  - Surface catalysis effects
- Shear layer and boundary layer transitional flows
  - Modeling tripping mechanisms associated with surface roughness, blowing, vibration and freestream disturbances
  - Real gas effects
  - Shock interaction and pressure gradient effects
- Turbulent interacting flows
  - Developing turbulence models for separated regions of shock wave/turbulent boundary layer interaction
  - Modeling turbulence/flow chemistry/combustion interactions
  - Transpiration cooling and ablation
- Mixing and Combustion
  - 3D mixing of fuel injector systems
  - Ignition and ignition delay aerothermodynamics
  - Mixing and combustion including shock interaction phenomena

Figure 2: Key Areas where Experimental Research is Required to Generate Accurate Design Techniques

In hypersonic flows, there are a number of key areas where the physical models in numerical prediction techniques must be improved and evaluated, as indicated in Figure 2. For laminar flows in the presence of real gas chemistry, the models of chemical nonequilibrium phenomena and radiation effects at velocities above 15,000 ft/s must be validated particularly in the area of vibration/dissociation coupling. The prediction of boundary layer and shear layer transition remains a major problem and experiment is required to evaluate real gas effects on these phenomena. The aerothermal loads developed during shock wave/turbulent boundary layer interaction cannot be predicted with any accuracy in hypersonic flows and when combined with combustion effects and active cooling, prediction of these flows becomes very difficult and the modeling employed in the prediction schemes require serious evaluation. For the design of ram and scramjet engines modeling of the 3D mixing phenomena associated with fuel injection systems, ignition and combustion of the fuel and the effects of shock interaction phenomena on engine performance remains to be investigated in experimental studies.

Knowledge of Boundary Condition	Flight Test Experiments	Ground Test Experiments
Probability of successful experiment	Poor – on first two flights Good – on subsequent flights	Good to excellent
Repeatability	None	Good to excellent
Knowledge of test conditions	Good – horizontal trajectory Good to poor – diving trajectory	Excellent – below Mach 8 Good to excellent – Mach 8 to 12 Good – Mach 12 to 24
Model attitude (⪤)	Poor to good	Excellent
Vehicle dynamics (coning and roll rate)	Good to poor – for spin stabilized flight	Excellent
Accuracy of surface measurements (heat transfer, pressure, skin friction, etc.)	Good to poor	Good to excellent
Accuracy of nonintrusive diagnostics	Good to poor	Good to excellent

Figure 3: Factors Influencing Accuracy of Flight and Ground Test Experiments

Flight test experiments are significantly more risky and the results are in general less accurate than the equivalent studies in ground test facilities (see Figure 3). Apart from the poor chances of obtaining good data in the first few flights, all the instrumentation is lost. Accurately defining the test environment is generally poor. A major reason for performing flight test experiments is to obtain an environment that is “clean” in respect to the turbulence level in the freestream and any effects of

nonequilibrium flow chemistry. In general, the scale of the vehicle employed in the flight test experiments can be replicated in today's large scale ground test facilities. The major drawback in flight test experiment is launch and vehicle cost and the total loss of all instrumentation.

3.0 REQUIREMENTS FOR GROUND TEST SIMULATION IN HYPERSONIC/HYPERVELOCITY FLOWS

Figure 4 illustrates that the requirements for ground test simulation in hypersonic/hypersonic flows generally vary with the object of the study. In a number of cases, the vehicle stability and aerothermal loads can be evaluated in a low enthalpy facility by simulating the Mach number and Reynolds number of the flow coupled with the wall to total temperature ratio. Also, studies of stores and stage separation may be conducted in low enthalpy flows. However, investigating real gas effects and evaluating airbreathing propulsion systems must be conducted under fully duplicated flight conditions with full-scale test articles. Materials and heat sink testing of the ablative components of hypersonic vehicles have traditionally been tested in arc jet facilities whose flows in general are not suitable for aerothermal/nonequilibrium flow studies.

	VEHICLE LOADS/ STABILITY	AEROTHERMAL LOADS	REAL GAS CHEMISTRY EFFECTS	AIRBREATHING PROPULSION	SHROUD, STORES, STAGE SEPARATION	MATERIALS AND STRUCTURES TESTING
TESTING REQUIRE-MENTS	Lift Drag Pitching Moment	Distribution of heat transfer, skin friction and pressure	Evaluate flowfield characteristics, heating and vehicle stability	Thrust, drag and aerothermal loads	Vehicle and component trajectory	Ablation, thermal management and structural integrity
TYPICAL MEASURE-MENTS	Surface pressure. Vehicle and component forces. Schlieren.	Pressure Heat transfer Skin friction Schlieren	Heat transfer Pressure Laser diode composition Temperature Velocity	Pressure, heat transfer, flowfield diagnostics Thrust measurements	High-speed photography, surface heat transfer and pressure Accelerometer measurements	Surface heating, recession, high speed Schlieren photography
PARAMETERS DUPLICATED	Mach Number/ Reynolds Number	Mach Number/ Reynolds Number T_{wall}/T_0	Mach Number Total temperature Density times length	Mach Number/ Reynolds Number Temperature Pressure Velocity Scale	Mach number/ Reynolds number Dynamic pressure	Thermal loads Flow temperature
PARAMETERS RELAXED	Total temperature. Flow Chemistry.	Velocity Flow Chemistry	Length	None	Velocity Temperature Vehicle length	Flow velocity Reynolds number Mach number
FLOW DURATION	10 Milliseconds – Minutes	5 Milliseconds – **Minutes**	100 microseconds – **50 Milliseconds**	> 5 milliseconds – Seconds	20 ms – 100 ms Minutes	Minutes

Figure 4: Ground Test Simulation of Hypersonic Flight

The requirements for simulation of viscous interaction and real gas phenomena in hypersonic flows are best shown in terms of a velocity/altitude chart similar to that presented in Figure 5. As illustrated in this figure, real gas and nonequilibrium flow phenomena are present in flows above 6,000 ft/s and can significantly influence the performance of existing and developing hypersonic vehicles. The pressure and temperature requirements to generate such flows are shown in Figure 6 for hypersonic facilities where the flow is expanded from stagnation conditions in the reservoir of the tunnel. For velocities of above 12,000 ft/s the pressure and temperature requirements are such that it is impossible to contain such a stagnation environment longer than 100^{th} of a second without significant damage to the reservoir region of the facility. Above 15,000 ft/s, not only is it extremely difficult to develop the temperatures and pressures required to directly simulate the flight environment, the properties of the gas in the reservoir and the gas expanded to freestream conditions are not well known and for most testing constitute a significant departure from the gas encountered by a flight vehicle traveling at these velocities.

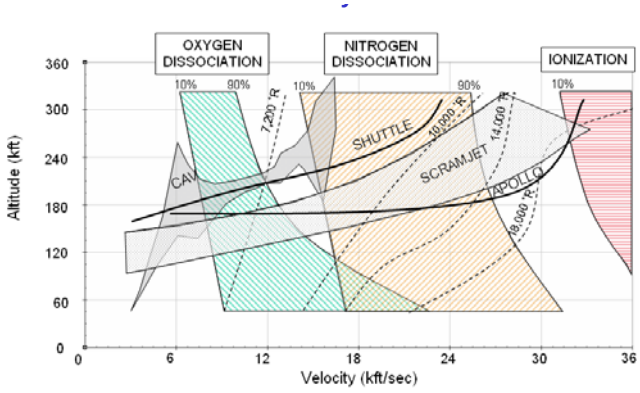

Figure 5: Velocity/Altitude Trajectory of Hypersonic Airbreathing and Re-entry Vehicles

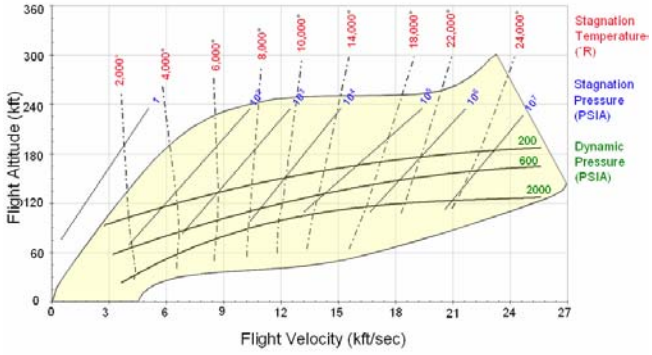

Figure 6: Reservoir Pressure and Temperature Requirements for Hypersonic Facilities

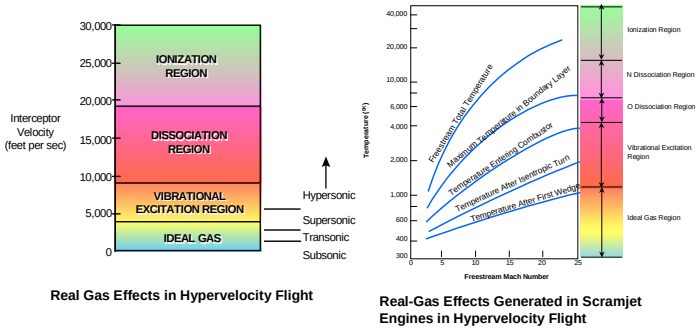

Figure 7: Temperatures Generated in Hypervelocity Flows

Again, as illustrated in Figure 7, the temperatures generated in hypervelocity flows can have a significant effect on scramjet performance and the performance of control and guidance systems for interceptors travelling at velocities above 8,000 ft/s.

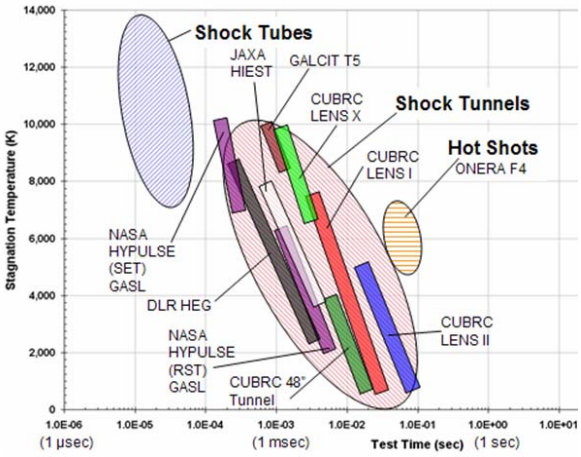

Figure 8: Hypervelocity Ground Test Facilities for Real Gas Studies

Figure 8 shows a compilation of the performance of high-enthalpy facilities capable of studying the aerothermal and nonequilibrium flow characteristics of hypersonic vehicles. The majority of the facilities in this plot are reflected shock tunnels whose driver sections employed either electrically heated hydrogen or helium (LENS I and II), piston heated helium (HIEST, HEG), or a combustible gas (HyPulse) to drive the incident shock. The two expansion tunnels (LENS X, HyPulse SET) employ heated hydrogen and combustion in the driver sections of the tunnel. The F4 Hot Shot tunnel employs an electrical discharge to heat the test gas and the resultant fluid can be contaminated in such a way that studying vibrational and chemical nonequilibrium effects in these flows is difficult. Generally the short duration of the flow generated in shock tubes is such that it is not possible to successfully study complex flow phenomena involving shock waves, combustion and wake flows.

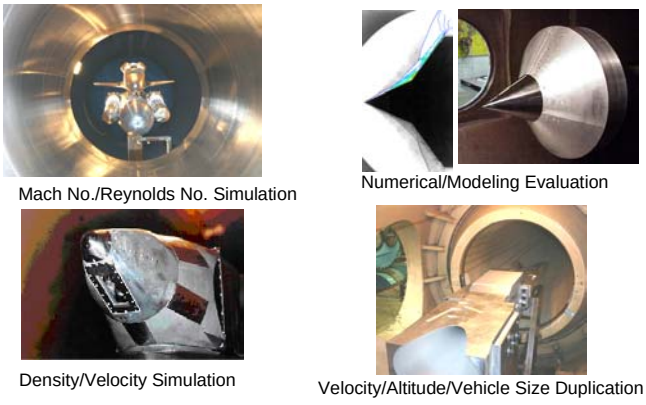

Figure 9: Simulation Requirements to Evaluate the Performance of Numerical Code/Models and Hypersonic Airbreathing and Re-entry Systems

The use of wind tunnels to generate information with which to evaluate vehicle performance to improve and validate prediction methods for hypersonic vehicle design can be divided into four classes of simulation as illustrated in Figure 9. Most aerothermal testing that has been performed in support of the design of vehicles like the space shuttle has basically employed Mach number/Reynolds

number simulation, testing without duplicating the total temperature of the flow but in some cases matching the wall-to-freestream stagnation temperature ratio. In these tests, the important measurements are pressure and heat transfer distributions, and the major phenomenon which must be replicated is the position of transition on the vehicle thereby ensuring heating levels can be related to those encountered in flight in terms of the appropriate Stanton number and Reynolds number of the flow. Of course, experiments to evaluate the performance of various numerical prediction schemes and the modeling employed in them can be performed in many ways as long as the key mechanisms of interest are correctly handled in the selection of test conditions. There are some tests for which the requirement to match altitude can be loosened to obtain density/velocity simulation. However, again for aerothermal tests, the position of transition on the body must be replicated to accurately obtain the heating loads. Also, in studies of the performance of seekerheads similar to those shown in Figure 9, it is important to replicate the turbulent characteristics of the turbulent boundary/shear layer flow over the window. To accurately evaluate the performance of scramjet-engine powered hypersonic interceptors, it is of key importance to duplicate not only the velocity/altitude conditions but also the size of the vehicle in order to obtain accurate aerothermal loads and vehicle thrust performance.

4.0 MACH NUMBER/REYNOLDS NUMBER SIMULATION AND AEROTHERMAL TESTS FOR SHUTTLE

As discussed above, the majority of tests conducted to evaluate the performance of hypersonic vehicles or to investigate and evaluate prediction methods have employed Mach Number/Reynolds number simulations. Compilations of the Mach Number/Reynolds Number capabilities of large-scale American and European hypersonic ground test facilities are shown in Figure 10. Also shown on this figure is a line drawn at a Reynolds number of 7 million which typically represents the requirement to obtain turbulent flows on models whose dimensions are two foot or larger. Clearly, in the high Mach number regime, there are few tunnels that are capable of generating fully turbulent flows without tripping, and tripping laminar boundary layers at Mach 8 is also difficult because of the large hysteresis effects in these flows.

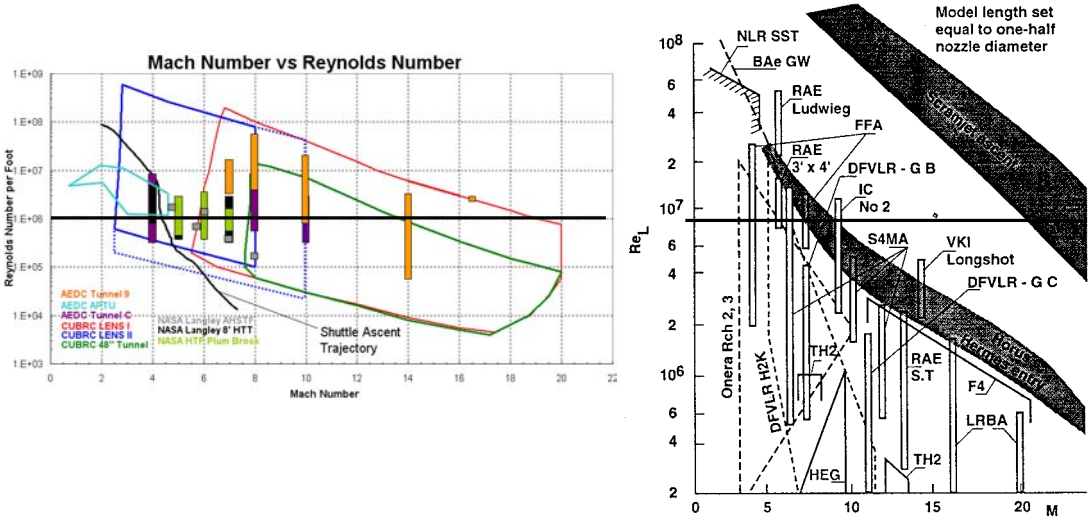

Figure 10: Mach Number/Reynolds Number Capabilities of American and European Hypersonic Ground Test Facilities

Many of the studies to evaluate the aerothermal performance of NASA and DoD vehicles have been performed to match not only the Mach number/Reynolds number of the flow but to also match the boundary layer to model length characteristics by matching the ratio of the wall temperature to the

recovery temperature. This is particularly important in the scale of viscous/inviscid interaction regions over control surfaces and in regions of shock impingement that are to be accurately scaled (see Figure 11).

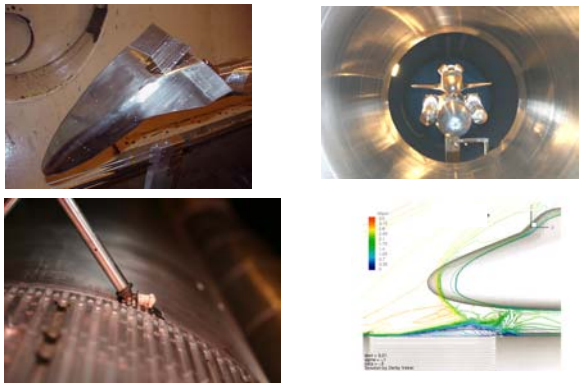

Figure 11: Mach Number/Reynolds Number, T_{wall}/T_0 Simulation for Aerothermal Studies on Hypersonic Re-entry Vehicles

In many ground test facilities selecting the model size and placing it accurately in the core flow is achieved most efficiently by computations to describe the flow characteristics around the model and in the test section as illustrated in Figure 12. This is of key importance where large models are required and the model can be positioned upstream of the nozzle exit in exploiting the uniform flow regions both upstream and downstream of the exit plane.

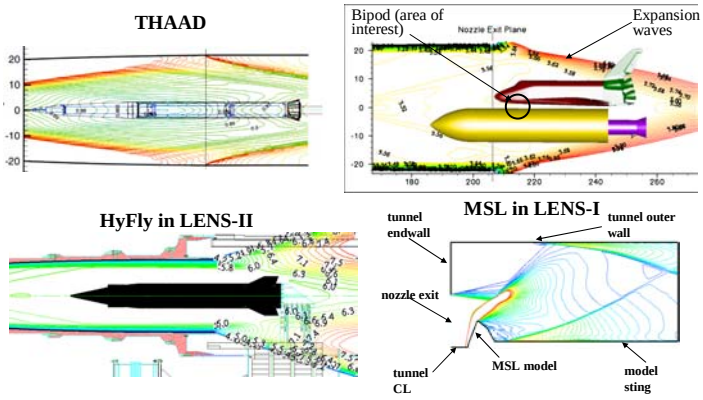

Figure 12: Computer Simulation of Nozzle Flows in Support of Ground Test Program

Also in the design of experimental studies, advanced computer solutions of the flow over the body are employed to select the stagnation temperature of the flow, test conditions and the positions of the instrumentation as illustrated in Figure 13. Each set of flow calibrations conducted with the survey rake similar to that shown in Figure 14 is matched with a computer solution of the entire flowfield initiated in the reservoir region of the facility. Comparisons between measured and predicted flowfield characteristics are illustrated in Figure 14. For low density flows, where viscous/inviscid interaction is of key importance, matching the rarefaction parameter is one way of simulating these flows. A compilation of the European capabilities to match rarefaction parameters is shown in Figure 15.

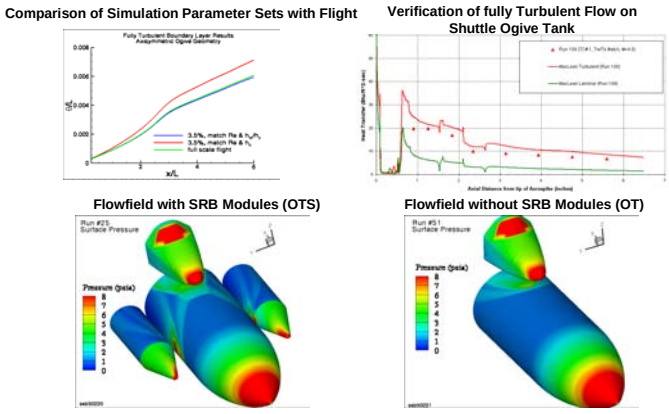

Figure 13: Numerical DPLR Simulations to Support the Test Condition Selection and Instrumentation Placement

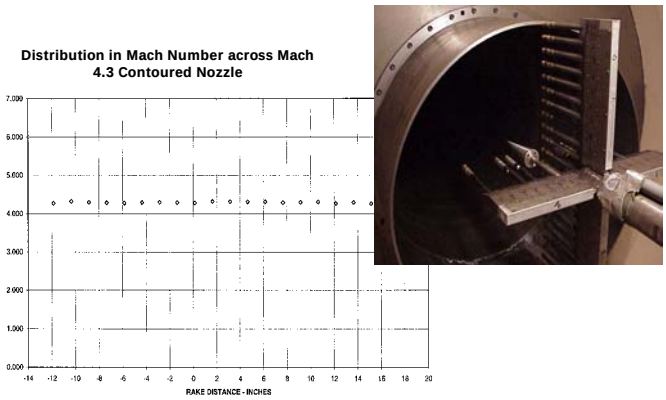

Figure 14: Flowfield Calibration in LENS II Test Facility

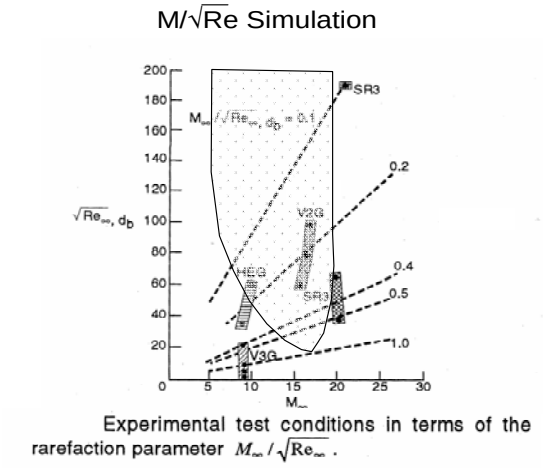

Figure 15: Rarefaction (M/√Re) and Density x Length (ρL) Parameters for Re-entry Simulation

These parameters are important in evaluating the high altitude aerothermal characteristics of vehicles like the X37 and X38 as illustrated in Figure 16 where the capabilities of the LENS facility is compared with the X37 trajectories plotted in terms of the rarefaction parameter and Mach number of the flow.

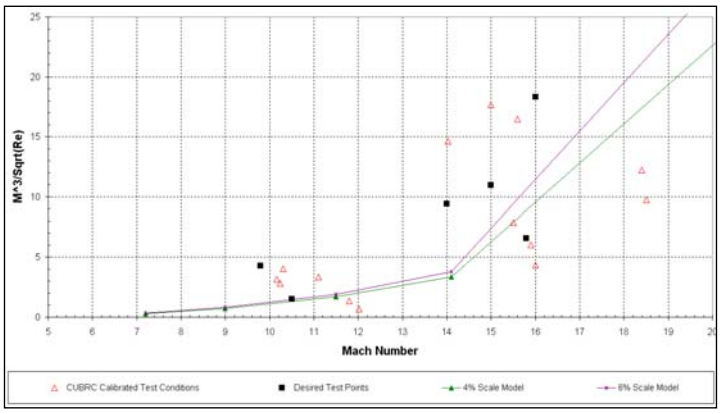

Figure 16: Viscous Interaction Parameters for X37 Vehicle

5.0 GROUND TEST FACILITIES TO EXAMINE REAL GAS EFFECTS IN HYPERVELOCITY FLOWS MAJOR HEADING HERE

To examine real gas effects in ground test facilities it is necessary to duplicate the velocity at the altitude of interest or, assuming that the chemistry is controlled primarily by binary scaling, replicate the binary scaling parameter ρL. For code validation studies, one can relax some requirements by duplicating the velocity and density of the freestream. However, for investigating flight vehicle performance of, for example, scramjets, it is necessary to duplicate the viscous environment, the nonequilibrium of the freestream, and the combustion process which requires full-scale test articles run at duplicated velocity/altitude conditions. A compilation of the ground test facilities capable of studying real gas effects are shown in Figure 17 in terms of the capabilities to generate duplicated velocity/altitude conditions. For small facilities where full-scale vehicles cannot be employed,

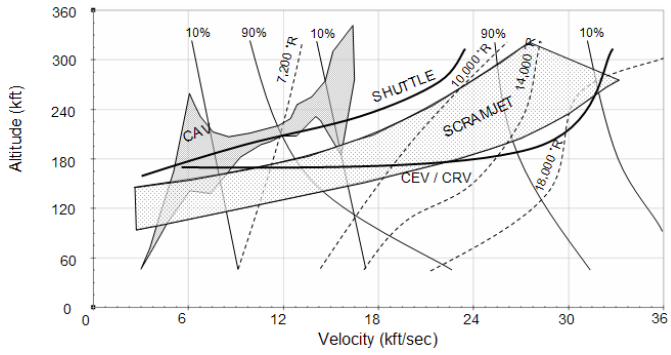

Figure 17 Hypervelocity Ground Test Facilities for Real Gas Studies

6.0 VELOCITY DENSITY SIMULATION FOR THE EVALUATION OF HYPERSONIC VEHICLE PERFORMANCE

For flows where real gas effects and combustion can have a significant effect on hypersonic vehicle performance it is necessary to duplicate the total enthalpy, density and pressure to obtain meaningful results. Examples of such flows are shown schematically in Figure 35 for flows associated with lateral thrusters employed in hypersonic interceptors, the flow over a seekerhead where an infrared sensor is employed to detect an oncoming missile, and in the scramjet engine where both real gas and combustion effects are of major importance. Because of the relatively small size (~12 ft) of the kill vehicle of a hypersonic interceptor it is possible to test a full-scale vehicle at fully duplicated conditions in a large hypersonic test facility.

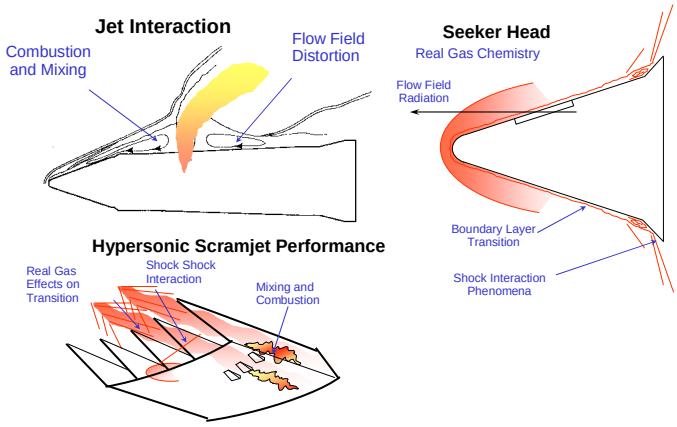

Figure 35: Flows where Total Enthalpy, Density and Pressure must be Duplicated – Real Gas Effects

Examples of two interceptor kill vehicles, the Army's AIT interceptor and the Navy's Standard Missile BLK IVA interceptor, are shown in Figure 36 together with a schematic of the IR instrumentation employed to examine the shock layer radiation to the seekerhead.

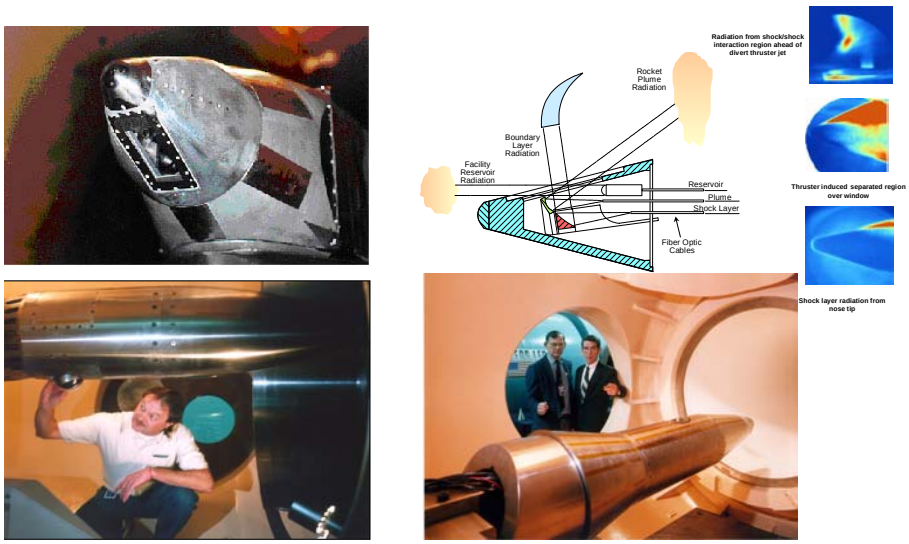

Figure 36: Aerothermal and Aero-optical and Radiation Studies of Full-Scale Interceptor Seekerheads/Kill Vehicle

Aerothermal and aero-optical studies were conducted with a full-scale replica of the Navy's Standard Missile BLK IVA under Mach 4 conditions to evaluate the effectiveness of the dome cooling system and determine the aero-optical performance of the seekerhead situated in the dome as shown in Figure 37. The aerothermal studies were conducted with the Standard Missile heated to flight temperatures using electrical heating techniques in both the missile body and dome as illustrated in Figures 38 and 39. The dome temperatures varied from room temperature to the recovery temperature of the flow in order to determine the heat transfer coefficient and the recovery temperature distribution for a range of vehicle attitudes and coolant heating rates.

Figure 37: Aerothermal Studies with the Full-Scale Navy Standard Missile BLK IVA

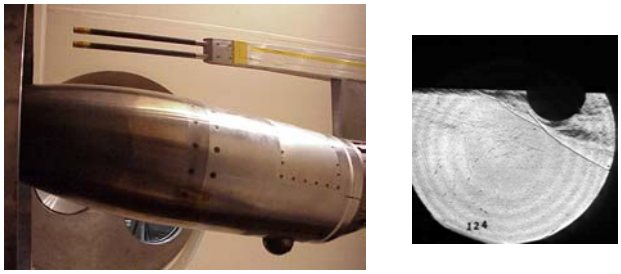

Figure 38: Aerothermal Testing with the Standard Missile BLK IVA Heated to Flight Temperatures

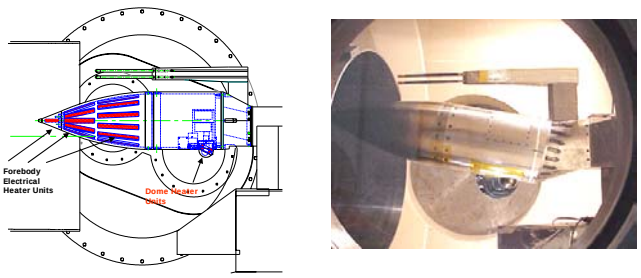

Dome Heating System **Missile installed in LENS II**

Figure 39: Standard Missile Heated Electrically to Flight Temperatures

The dome was highly instrumented with high-temperature heat transfer gages as illustrated in Figure 40. The distribution of heat transfer measured with this instrumentation around the dome is also illustrated in this figure. Figure 41 illustrates the method of analysis and typical recovery temperature and heat transfer coefficient distribution which were obtained in these studies.

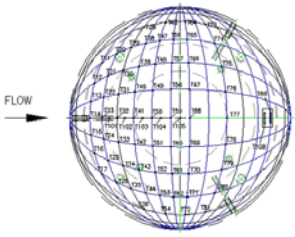

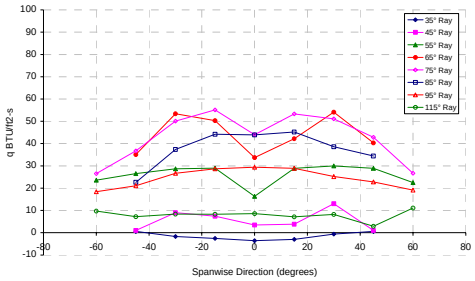

Figure 40: Measurements of Heat Transfer, Recovery Temperature and Heat Transfer Coefficient with a Heated Standard Missile Dome

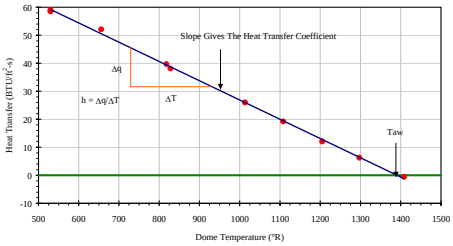

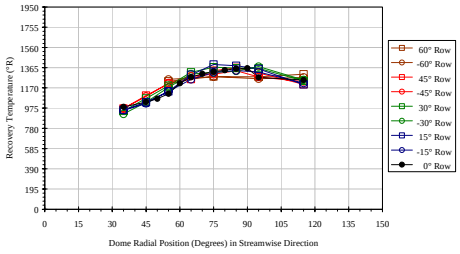

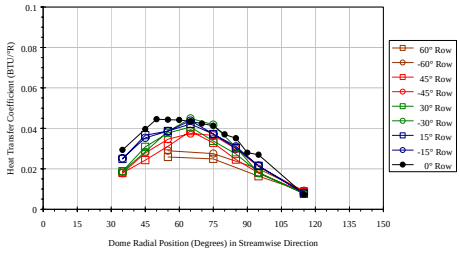

Figure 41: Analysis of Heat Transfer Measurements to Obtain Recovery Temperature and Heat Transfer Coefficient

Most windows on seekerheads of interceptors to be flown at hypersonic velocities employ active cooling and this active cooling system can cause significant aero-optic distortions potentially limiting the performance of the seekerhead. Typically helium is employed as a coolant gas both to match the freestream velocity and because of its low reflective index to minimize the optical distortions. Figure 42 illustrates why it is important to match the total enthalpy/velocity and density to replicate the mixing flow over the windows and hence the aero-optic distortions. If tests are conducted in a low enthalpy facility, both the coolant effectiveness and the aero-optic distortion cannot be evaluated with any accuracy whatsoever.

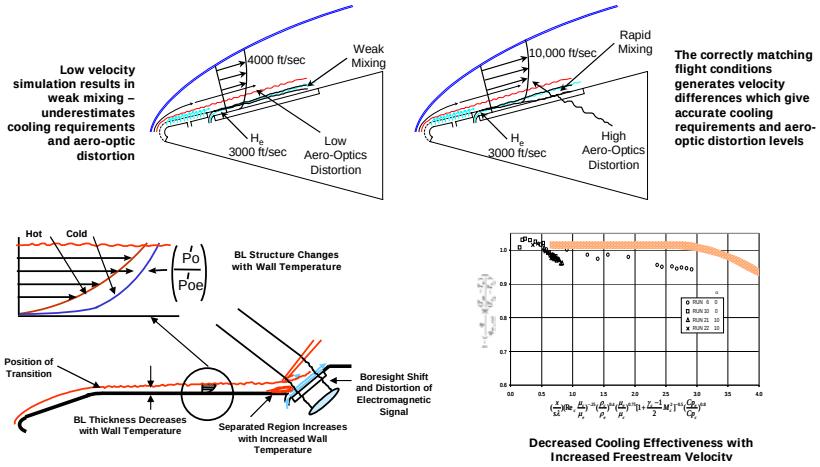

Figure 42: Total Enthalpy and Density must be Duplicated to Replicate Mixing and Aero-Optic Distortion Effects

Figure 43 shows a number of seekerhead window configurations tested at full scale at fully duplicated flight conditions in the LENS I tunnel at CUBRC. All of these configurations employ active window film cooling, although in the Lockheed seekerhead the coolant is contained within the seekerhead window. Obtaining accurate aero-optical data to evaluate image distortion and boresight shift through the film cooled window is an extremely difficult task. To obtain measurements of boresight shift within an accuracy of 10 microradians requires an aero-optic evaluation suite which is integrated with the tunnel (see Figure 44) so that the optical bench system is understood during the operating time of the wind tunnel.

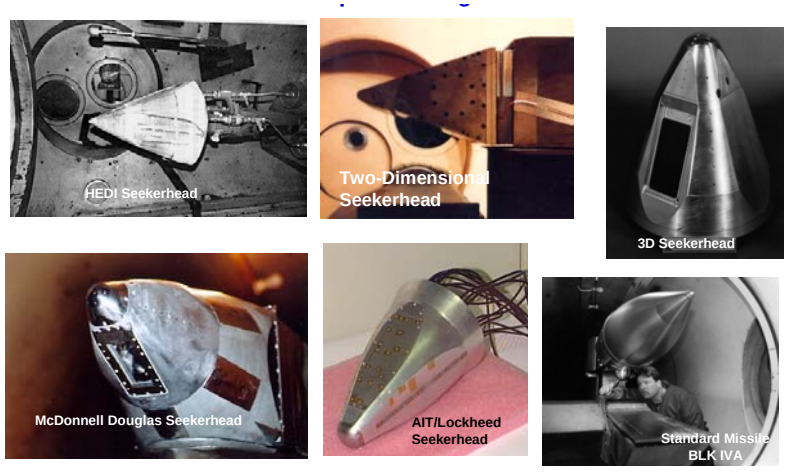

Figure 43: Aerothermal and Aero-optical Studies with Full-Scale Seekerheads at Duplicated Flight Conditions

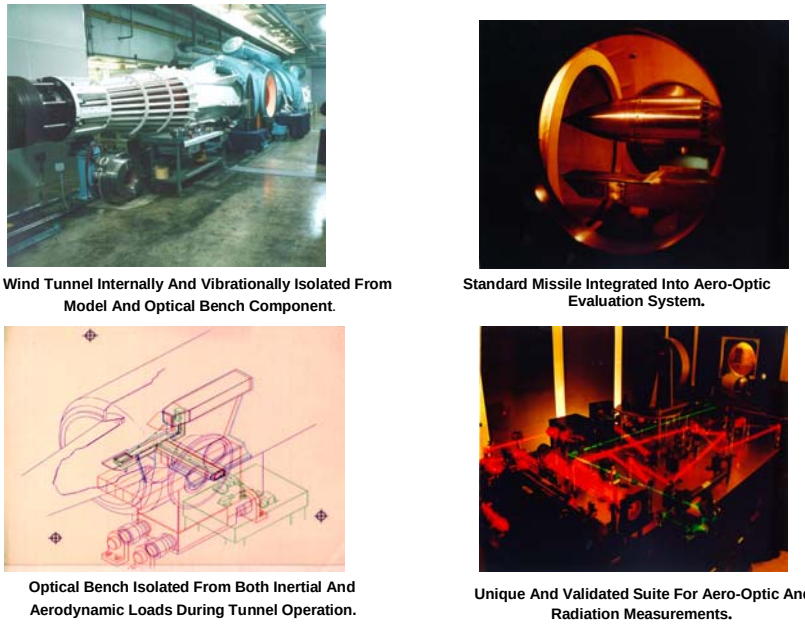

Figure 44: Wind Tunnel and Aero-Optic Suite: A Totally Integrated Key Design Feature

Examples of measurements obtained to evaluate optical distortion, boresight error shift, and boresight error slope are shown in Figure 45.

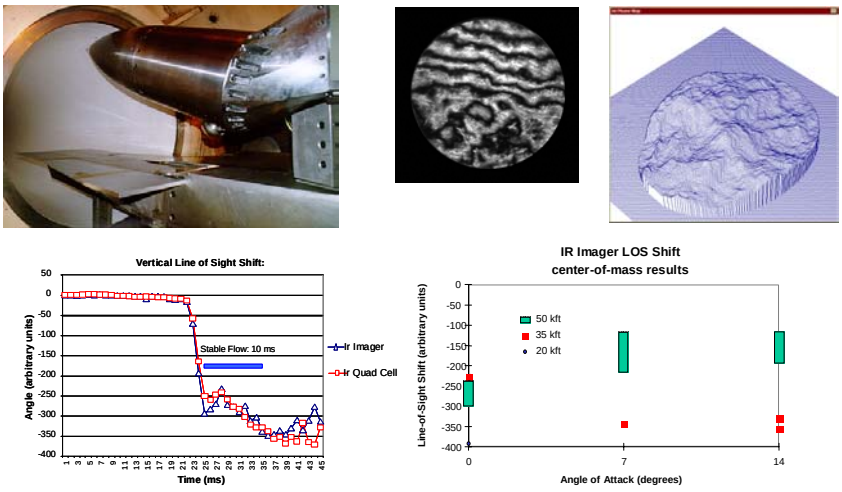

Figure 45: Aero-Optic Studies with High-Speed Interceptor at Angle of Attack for Low Look Angles

In these studies we measured the aero-optic distortion associated with the external flow over the window; however, we also obtained measurements of the distortion through the window itself as it is heated by imposing an impulsive heat load as illustrated in Figure 46.

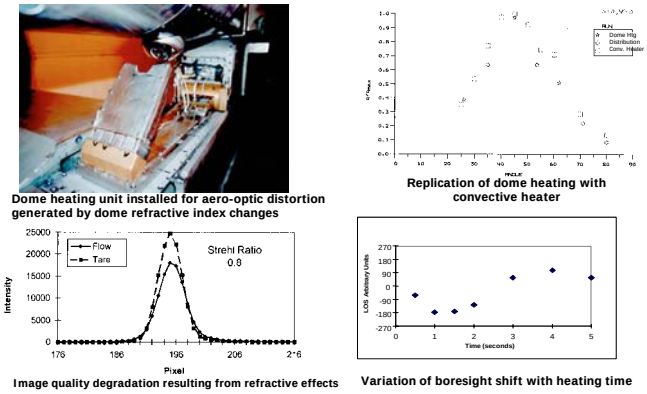

Figure 46: Measurements of Aero-Optic Distortion associated with Changes of the Refractive Index of the Heated Dome

These programs were conducted to evaluate seekerhead configurations designed to be operated in the atmosphere; however testing can also be conducted to evaluate seekerhead performance in low density flows associated with exo-interceptors similar to the LEAP configuration shown in Figure 47.

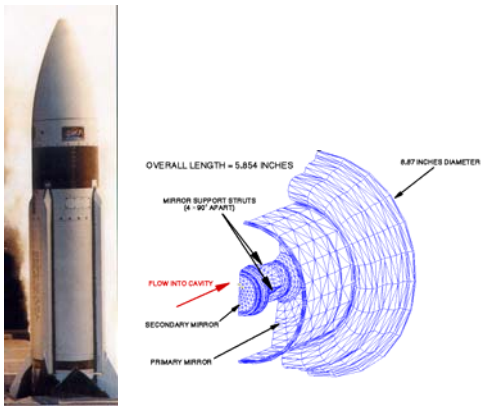

Figure 47: Low Density Studies of the LEAP Seekerhead

These studies were principally oriented toward measuring the heating loads on the seekerhead and validating the DSMC prediction techniques employed in their design. Typical full and subscale models of this configuration are shown in Figure 48.

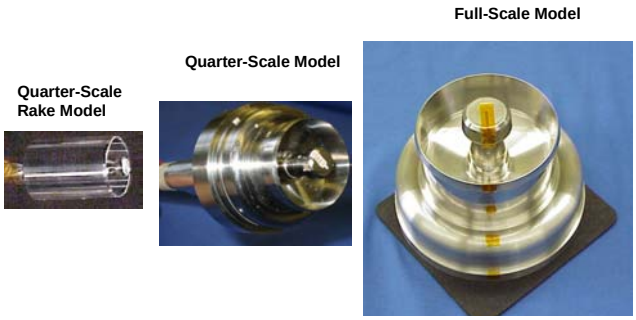

Figure 48: Design, Construction and Instrumentation of Seekerhead Models

6.1 Studies of Jet Interaction Phenomena Associated with Divert Thruster Performance

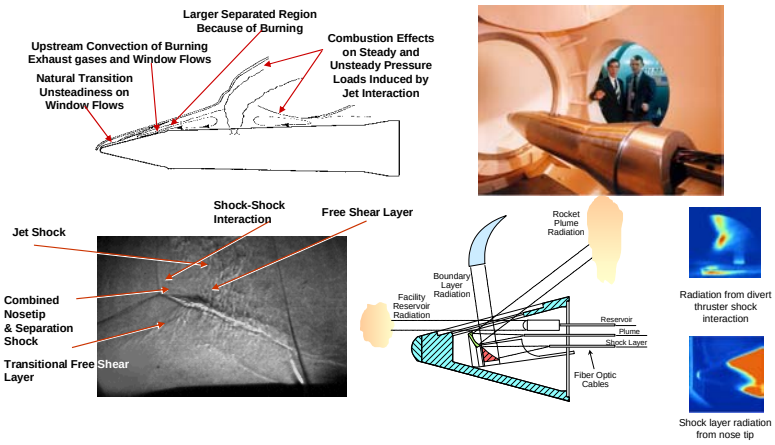

Figure 49: Aerothermal and Radiation Studies of Divert Thruster Performance with Duplicated Vehicle and Solid Propellant Rocket Motor

Divert thrusters provide the major control system for an endo-interceptor kill vehicle; however, the rocket motors which are employed in the divert thruster can generate significant interaction phenomena which can have major effects on the jet interaction forces and the flowfield ahead of the thruster and over the seekerhead window as illustrated in Figures 49 and 50. Also shown in Figure 49 are the IR measurement systems employed to determine the shock layer radiation and provide images of the burning shear layer and shock interaction phenomena which occur over the vehicle.

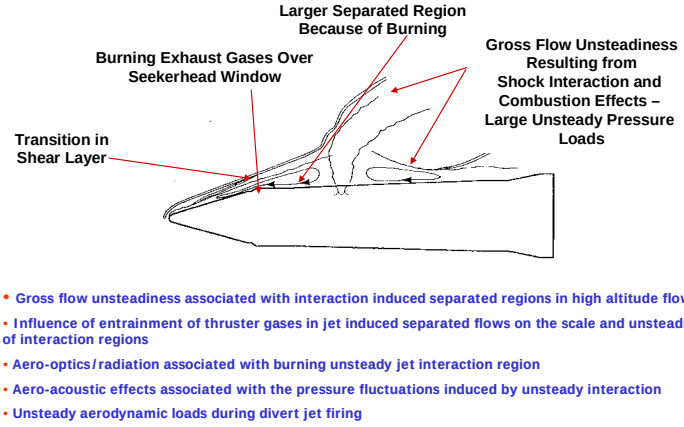

Figure 50: Key Flow Phenomena and Critical Issues for Flight and Ground Testing of Divert Thrusters

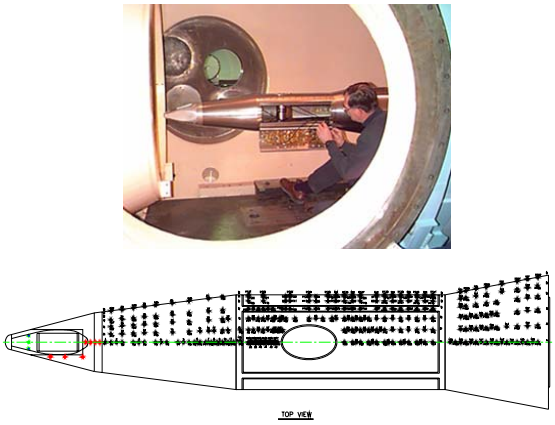

Figure 51: AIT Kill Vehicle Densely Instrumented with Heat Transfer and Pressure Gages

In order to obtain accurate information of the mean and fluctuating flowfield over such configurations, detailed time resolved pressure and heat transfer measurements must be made. Figure 51 shows the densely instrumented full-scale model of the AIT interceptor and measurements from these instruments are presented in Figure 52 for reacting and non-reacting interaction regions conducted by employing air and nitrogen, respectively, as the freestream gas.

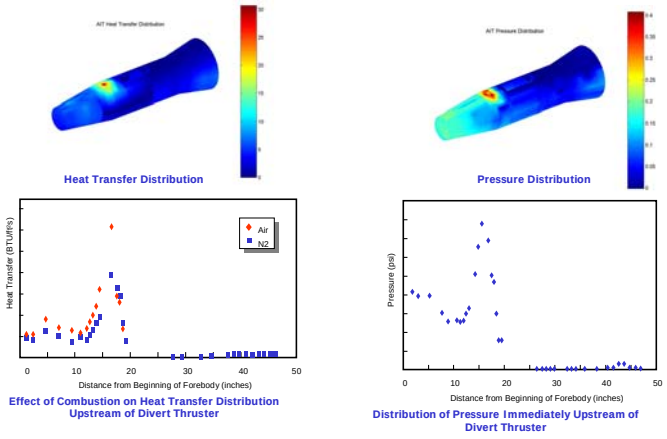

Figure 52: Measurements of the Heat Transfer and Pressure in the Jet Interaction over the AIT Kill Vehicle

Direct measurements of the forces generated by the divert thruster were also made using a high frequency force balance system similar to that shown in Figure 53. Also high-speed high-frequency acoustic instrumentation was employed to determine the loads transmitted to the seekerhead through the kill vehicle which resulted from the major unsteadiness of the flows ahead and behind the thruster as illustrated in Figures 54, 55 and 56. Computations of the unsteady nature of these flows were attempted using time-resolved Navier-Stokes prediction techniques (Figure 57). As mentioned earlier, radiation measurements were obtained both through the seekerhead window and from cameras situated outside the tunnels to evaluate the radiation characteristics of the flows over the seekerhead (Figure 58).

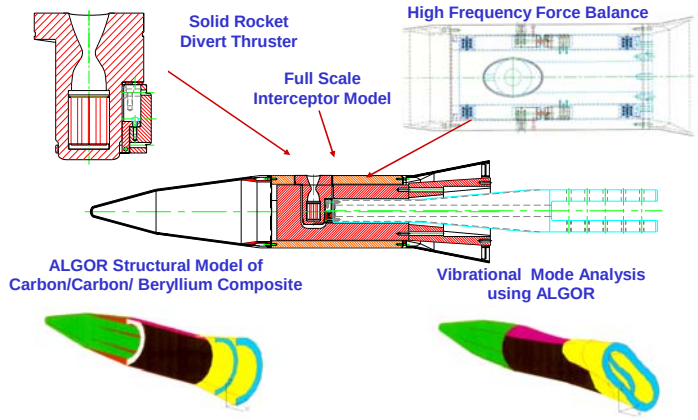

Figure 53: Force Measurements of Jet Interaction Effects at Duplicated Flight Conditions

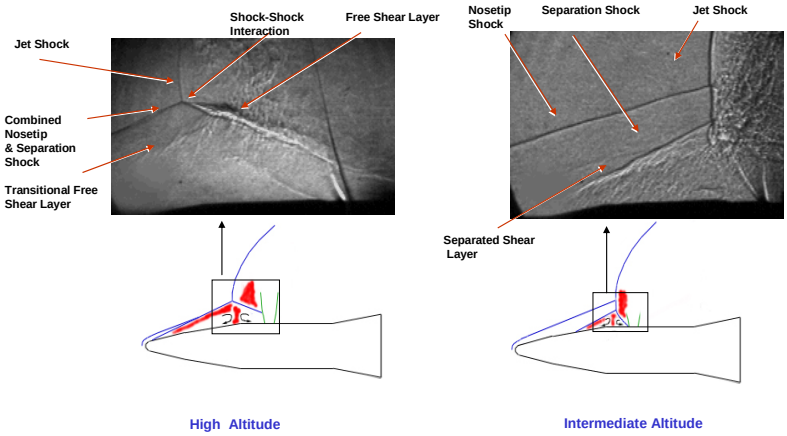

Figure 54: Schlieren Photographs of Jet Interaction

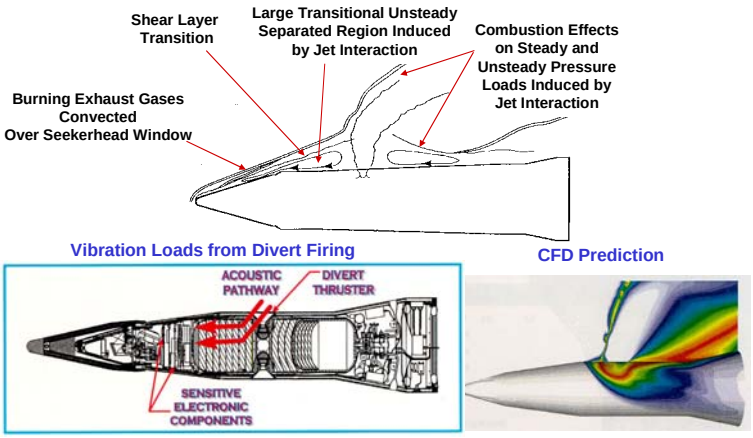

Figure 55: Large Unsteady Pressure Loads Creating Acoustic Problems with Infrared Seeker

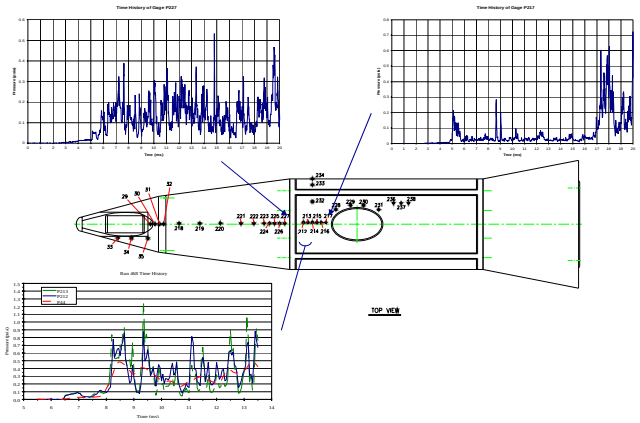

Figure 56: Unsteady Pressure Loads ahead of Divert Thruster

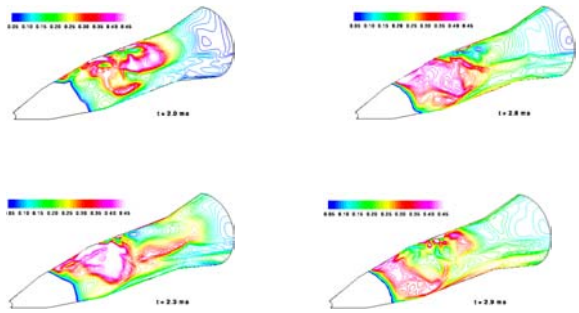

Perrell, E., and Dash, S.M., "Transient Simulation and Preliminary Data Comparisons for Interceptor Missile Divert Jet Interactions," presented at 2000 JANNAF EPTS & SPIRITS User Group Joint Meeting, Nellis Air Force Base,Las Vegas, NV, May 15-19, 2000.

Figure 57: Navier-Stokes Computations depicting the Unsteady Nature of the Interaction Region around the Divert Thruster

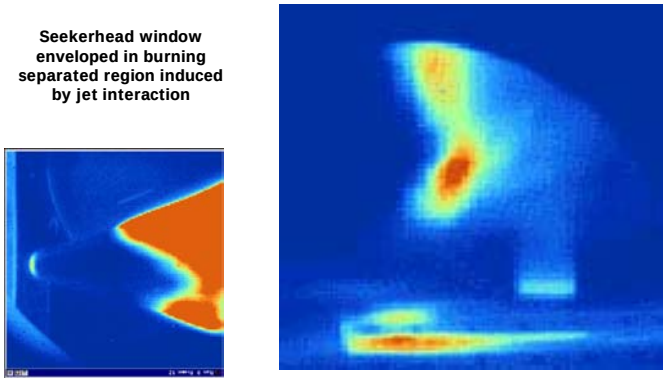

Figure 58: Infrared Radiation from Flow over Seeker Window and from Divert Thruster Flowfield

7.0 VELOCITY/ALTITUDE SIMULATION AND SCRAMJET ENGINE TESTING

To accurately evaluate the performance of scramjets the size typical of interceptors or prototypes such as the X43 and ARRMD, it is necessary to duplicate the flight environment and employ a full-scale test article. Only in this way can the complex flow in the inlet and isolator as well as the combustion process be accurately simulated. The large-scale vitiated air and shock tunnel test facilities currently available can accommodate full-scale vehicles. As illustrated in Figure 59, the X43, ARRMD and HyCause flight vehicles are shown positioned in the LENS II tunnel for testing at velocities from 6,000 to 11,000 ft/s.

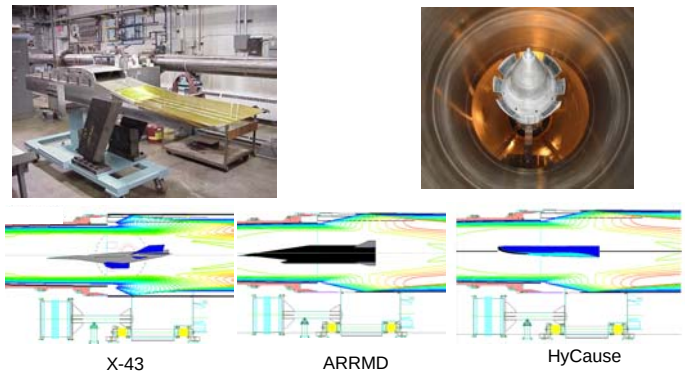

Figure 59: Velocity/Altitude Duplication for Full-Scale Scramjet-Powered Testing of Flight Vehicles

Figure 60 shows the key fluid dynamic, aerothermal and combustion phenomena which are encountered in a scramjet-propelled vehicle. In addition to real gas effects, these flows are influenced by boundary layer transition, shock boundary layer interaction, and mixing and combustion basically combining all of the phenomena which are difficult to predict in numerical codes.

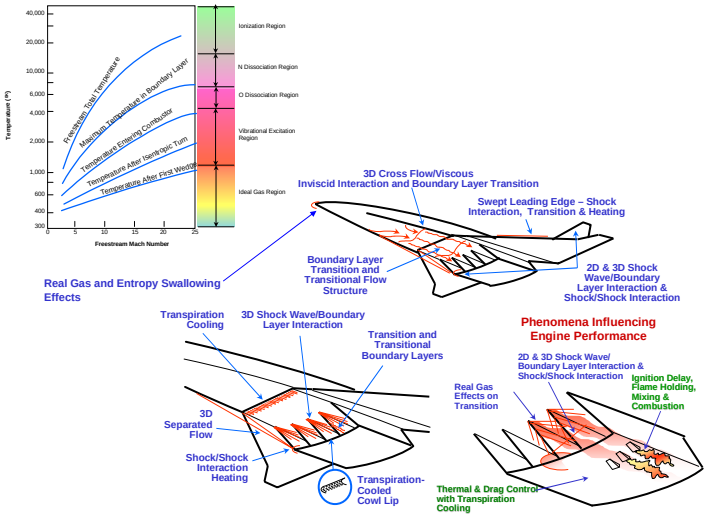

Figure 60: Key Aerothermal and Combustion Problems Associated with Scramjet Propulsion

Figure 61 shows the performance of large-scale ground test facilities which can be employed in the development of scramjet engines. Most scramjet testing is performed in intermittent or short duration test facilities. For the intermittent facilities, the hot gas is generated either by a combustion process or through electrically heating a pebble bed storage vessel. Because of energy requirements these facilities are limited in pressure and temperature performance at Mach numbers below 7. Flow vitiation also presents a problem in evaluating the contribution of combustion products on the ignition and combustion of the fuel inside the engine. Short-duration facilities, those with test times between 3 ms and 100 ms, have been employed to obtain clean air measurements from Mach 6 to 12 and have the additional advantage that high pressure can be generated allowing testing for dynamic pressures up to 3,000 psf. Although pulse facilities (test times <1 ms) have been employed to investigate combustion in a small scale engine, serious questions remain as to the effect of the short duration on the measurements in the combustor.

TEST TIME / TUNNEL PERFORMANCE	CONTINUOUS TIME ~ 1 min	INTERMITTENT TIME ~ 1 – 20 sec	SHORT DURATION TEST TIME ~ 3 - 100 mS	PULSE TEST TIMES <1 mS
	HEAT EXCHANGER	VISCIATED OR PEBBLE-BED HEATED GAS	LUDWEIG/ REFLECTED SHOCK TUNNELS AND EXPANSION TUNNEL	COMBUSTION/PISTON DRIVEN SHOCK TUNNELS EXPANSION TUNNELS
Maximum Reynolds Number at Mach 8	10^6	10^7	10^8	10^8
Stagnation Temperature/Velocity	2,000° R/ 2,000 ft/sec Electrical	4,000° R/ 5,000 ft/sec Electrical/ Combustion	15,000° R/ 14,500 ft/sec Electrical/ Shock Heated	25,000° R/ 28,000 ft/sec Shock Heated Expansion Accelerated
Test Gas	Air	N_2/Visciated Air	N_2 / Air	N_2/Components of Air N_2 / Air
Boundary Layer Condition	Laminar/ Transitional	Transitional/Turbulent →Mach 10	Turbulent → Mach 13	Laminar/ Transitional
Combustion and Reacting Jet	No	For Vitiated Air Facilities	Yes	Yes
Test Section Dimension	3 ft	8 ft	8 ft	8 ft
Flow Lengths $\left(\frac{t_{run} V_\infty}{d}\right)$ for 1 ft Combustor Length	> 1,000	> 1,000	10 – 100	1 – 30
Major Testing Facilities Supporting Scramjet Development	Not used for engine testing	GASL Johns Hopkins Wright Labs NASA Langley AEDC	CUBRC GASL/NASA	GASL/NASA Australian CUBRC German Caltech Japanese

Figure 61: Capabilities of Large-Scale Scramjet Ground Testing Facilities

Figure 62 shows a number of full-scale scramjet engines which have been tested in the LENS facility with full-scale vehicle and engine components. Most of these tests have been conducted in the LENS I facility at Mach numbers from 6 to 12, although a series of tests were accomplished with the HyCause and HyFly missile at Mach numbers between 3.5 and 6. Figure 62 shows photographs of these engines in these two tunnels.

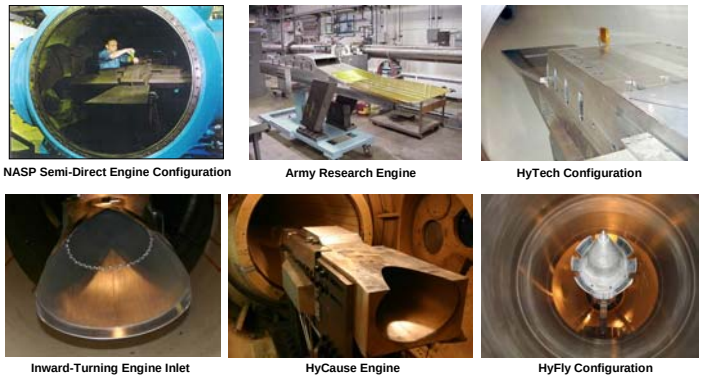

Figure 62: Scramjet Engines Tested in LENS Facility

Figure 63 shows the capabilities of the LENS tunnels to perform scramjet testing from Mach 3.5 to Mach 18. LENS X has not been used for scramjet testing. However, it has the capability to be employed in freejet and semi-freejet testing at Mach 15 and 20, respectively, as illustrated in Figure 64.

LENS I
Velocity Range (ft/sec)
3,000 – 15,000
Altitude (kft)
25 - 300
Mach Numbers
8.0 - 18.0
Reynolds Numbers (1/ft)
1.0E4 - 1.0E8
Test Time (ms)
up to 25
Nozzles
Mach 8 – 10 (48” Exit)
Mach 10 – 18 (48” Exit)

LENS II
Velocity Range (ft/sec)
2,500 – 9,000
Altitude (kft)
SL - 200
Mach Numbers
3.0 - 8.0 (Upgrading to 10)
Reynolds Numbers (1/ft)
1.0E5 - 1.0E9
Test Time (ms)
up to 100
Nozzles
Mach 3 – 5 (42” Exit)
Mach 5 – 8 (60” Exit)

LENS X
Velocity Range (ft/sec)
14,000 – 22,000
Altitude (kft)
120 - 250
Mach Numbers
14.0 - 22.0
Reynolds Numbers (1/ft)
1.0E3 - 1.0E6
Test Time (ms)
up to 4
Nozzles
Mach 14 – 22 (60” Exit)

Figure 63: LENS Propulsion Facilities to Investigate Ramjet/Scramjet Performance from Mach 3.5 to Mach 18

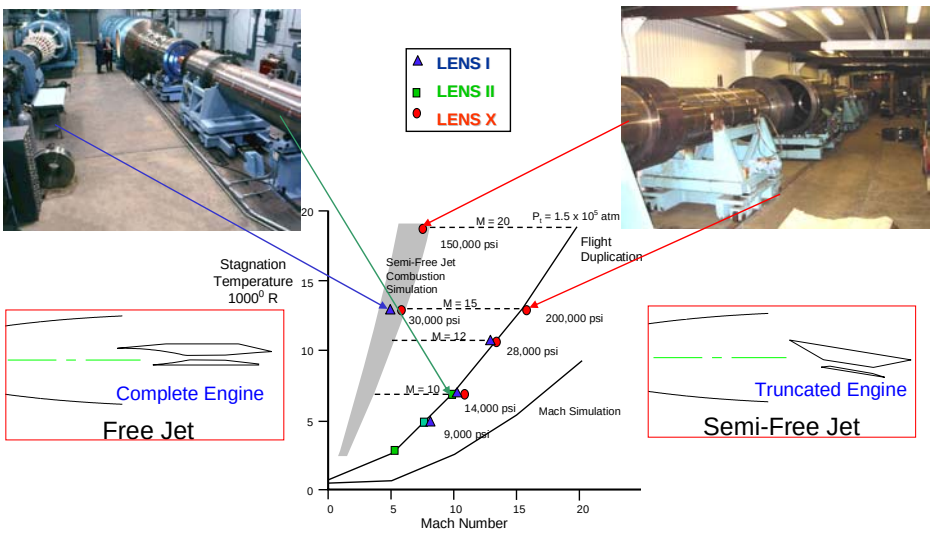

Figure 64: LENS Capabilities for Full-Scale Ground Tests

Figure 65 shows the velocity/altitude performance of large propulsion facilities in the U.S. including AEDC, which is employs a nitrogen test gas but can be used in inlet studies. Also shown in this figure are the range of test points at which scramjet testing has been conducted in the LENS I and II test facilities. These studies have covered vehicles from the NASP combuster to the current Army research engine

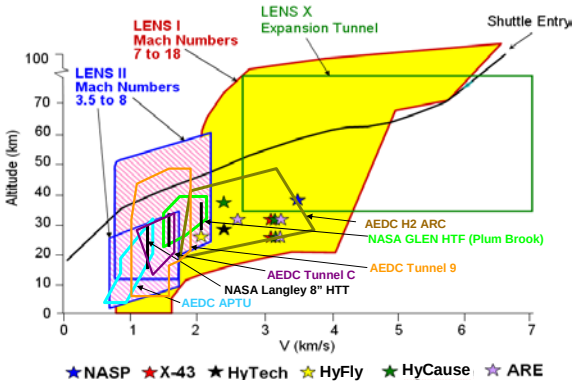

Figure 65: Velocity/Altitude Performance of LENS Tunnels and Other Large Propulsion Test Facilities

These engine configurations are shown in Figure 66. During the NASP program, semi-direct testing was performed at Mach 12 with the NASP combuster (see Figure 67). Similar tests were repeated in the LENS I facility. During this same period, an extensive set of code validation measurements were done to examine key aerothermal phenomena such as shock/shock interaction, transition on inlets, film and transpiration cooling, and flow relaminarization in the nozzle with the models shown in Figure 68.

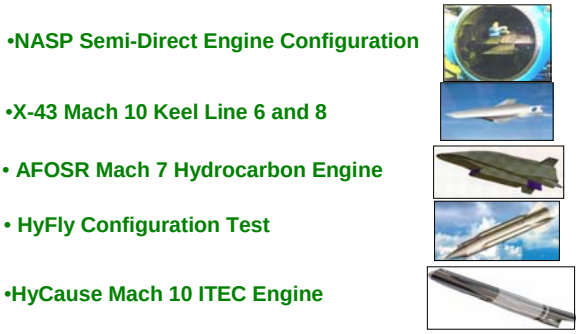

Figure 66: Full-Scale Engine Ground Test Evaluation of Contemporary Ram/Scramjet Designs at Fully Duplicated Flight Conditions

Figure 67: NASP Studies at Calspan

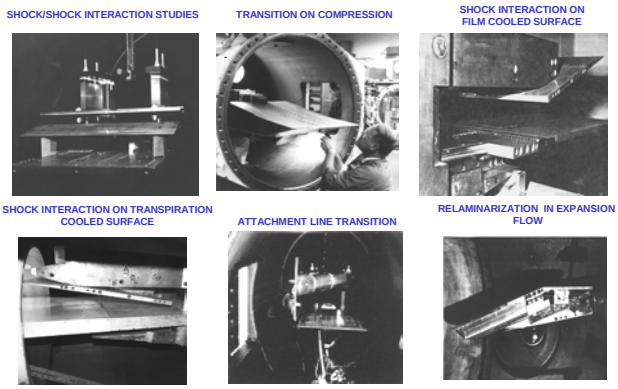

Figure 68: Studies of Fundamental Flow Phenomena for CFD Prediction/validation for NASP

Detailed heat transfer and pressure measurements were made in the NASP engine shown in Figure 69 for a range of Mach numbers from 8 to 12.

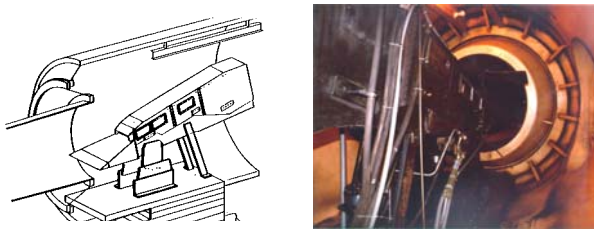

Figure 69: NASP Scramjet Engine tested in LENS I

Typical time histories of heat transfer and pressure instrumentation in the combuster are shown in Figure 70. Measurements were typically made over a 2 ms test window in the 8 ms flow length

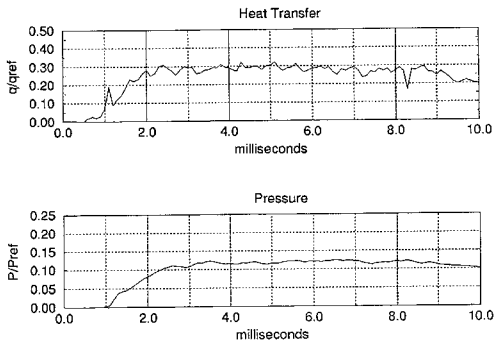

Figure 70: Typical Time Histories of Heat Transfer and Pressure for the Mach 12 Combustor Tests

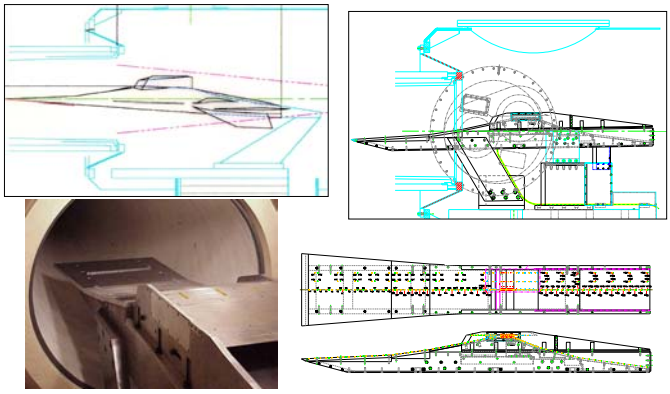

Figure 71: Testing of Full-Scale X-43 Flow paths [KL6 & 8] at Duplicated Flight Conditions

Tests were conducted with two full-scale flowpaths for the X43 engine for a range of dynamic pressures at the Mach 10 flight condition. Figure 71 shows the X43 configuration and the research engine in which the measurements were made.

Averages	P_0 (psia)	T_0 (°R)	M_∞	ρ_∞ (slugs/ft·s)	P_∞ (psia)	Q_∞ (psia)	T_∞ (°R)
Q=750	6358.90	6982.70	10.09	1.490E-05	7.440E-02	5.17	417.19
Q=1000	9226.92	7042.02	10.10	2.036E-05	9.936E-02	7.09	407.96
Q=1350	12306.17	7179.38	10.08	2.652E-05	1.327E-01	9.44	417.99

Q=750	M_∞	Q_∞ (psf)	P_∞ (psia)	ρ_∞ (slugs/ft·s)	V_∞ (ft/s)	T_∞ (°R)	Alt (kft)
X-43	10.00	750.00	7.442E-02	1.453E-05	10161.91	429.69	117.44
LENS	10.09	744.48	7.440E-02	1.490E-05	9996.51	417.19	117.44
% Diff	0.90	0.74	0.03	2.55	1.63	2.91	0.00

Q=1000	M_∞	Q_∞ (psf)	P_∞ (psia)	ρ_∞ (slugs/ft·s)	V_∞ (ft/s)	T_∞ (°R)	Alt (kft)
X-43	10.00	1000.00	9.919E-02	1.983E-05	10042.81	419.69	110.86
LENS	10.10	1020.93	9.936E-02	2.036E-05	10014.86	407.96	110.82
% Diff	0.98	2.09	0.17	2.66	0.28	2.80	0.04

Q=1350	M_∞	Q_∞ (psf)	P_∞ (psia)	ρ_∞ (slugs/ft·s)	V_∞ (ft/s)	T_∞ (°R)	Alt (kft)
X-43	10.00	1350.00	1.340E-01	2.735E-05	9936.25	410.83	104.15
LENS	10.08	1359.61	1.327E-01	2.652E-05	10125.17	417.99	104.35
% Diff	0.82	0.71	0.99	3.02	1.90	1.74	0.19

Figure 72: Comparison between X-43 Flight Conditions and LENS I Test Conditions

Figure 72 demonstrates the test conditions at which measurements were made and demonstrates the close simulation of the flight test conditions.

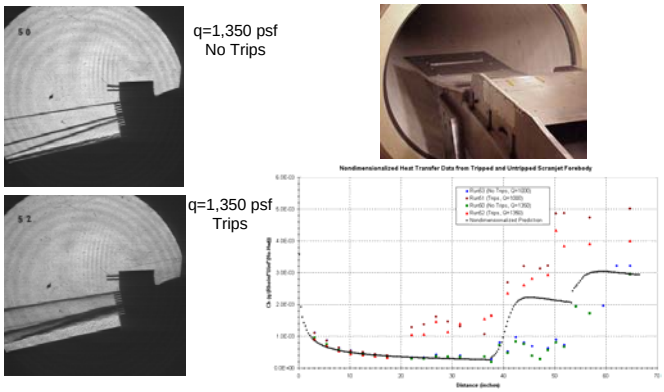

Figure 73: Effect of trips on Flow Pattern and Heating Over Inlet

During this test series, detailed studies were made of the flow over the inlet ramp with a range of trip configurations employing both Schlieren (Figure 73) and holography (Figure 80) to visualize and quantify the flowfield.

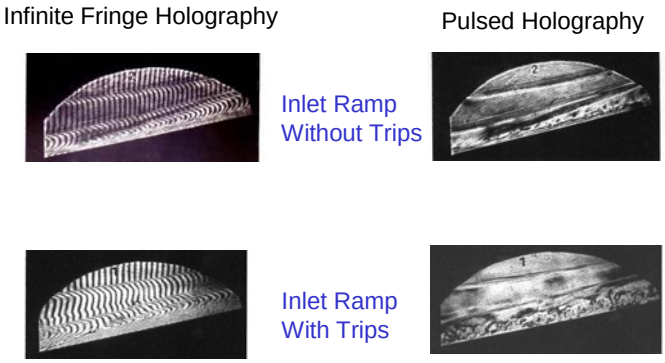

Figure 74: Flow Visualization with Infinite Fringe and Pulsed Holography

Detailed heat transfer and pressure measurements were made over the inlet and closed cowl configuration for a range of test conditions and model temperatures to examine boundary layer trip effectiveness and closed door heating (see Figures 74 and 75).

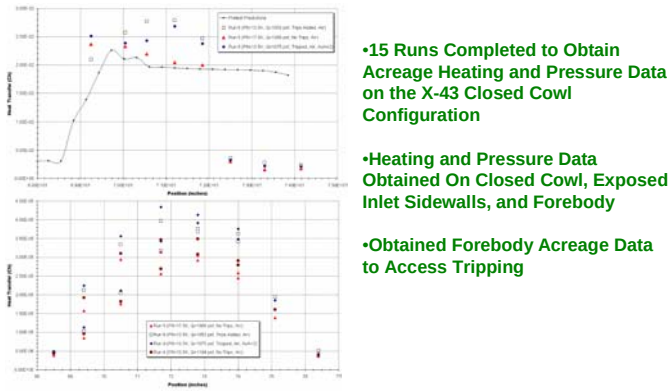

Figure 75: X-43 Closed Cowl Heating Investigation in LENS I

The Army generic engine was also employed in studies for AFOSR of a Mach 6 scramjet engine using both hydrogen and hydrocarbon fuels. Figure 76 shows the engine installed in the LENS I tunnel for these tests. An installation drawing of the model in the tunnel showing the heated Ludweig tube supply system is shown in Figure 77.

Figure 76: Model Configuration used for AFOSR Studies

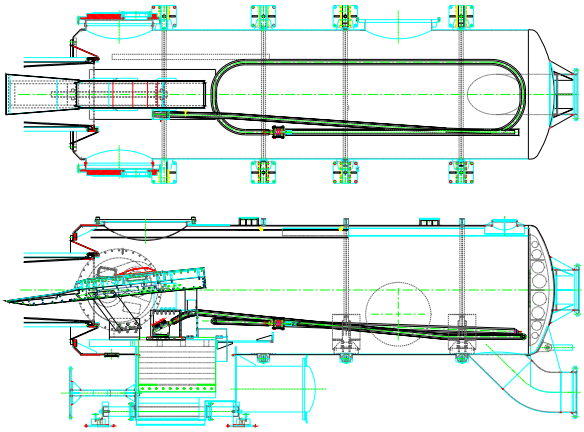

Figure 77: Heated Ludweig Tube Supply System for Scramjet Fuel

This engine was highly instrumented with piezoelectric pressure and thin-film heat transfer gages as shown in Figure 78.

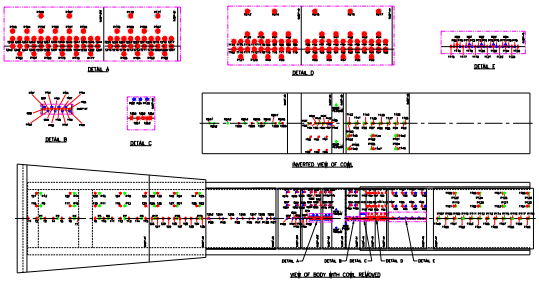

Figure 78: Instrumentation Layout on Generic Scramjet Engine

Typical sets of heat transfer measurements obtained for tare conditions and with hydrogen and hydrocarbon fuels are shown in Figure 79. Under both conditions we employed hydrogen/oxygen torch igniters situated in a cavity flameholder to initiate burning through the engine.

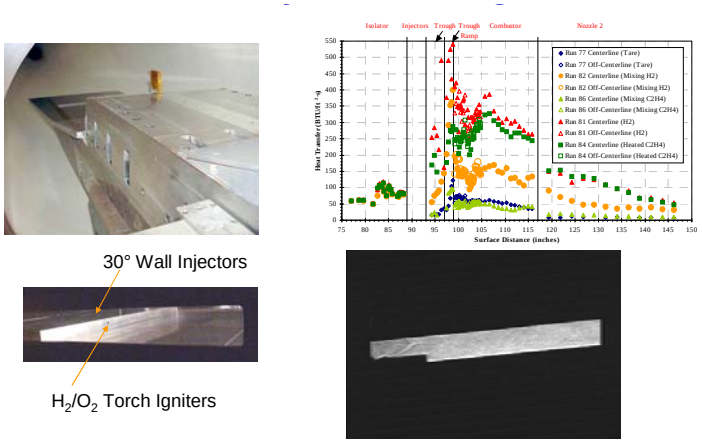

Figure 79: AFOSR Studies of Mach 7 Hydrocarbon Engine

Detailed aerothermal studies were conducted to develop the trip configurations for the HyFly vehicle and measure the interference and acreage heating over the complete vehicle. Figure 80 shows the full-scale HyFly configuration installed in the LENS I tunnel, the positions of the heat transfer instrumentation and typical measurements made downstream of the trip on the inlet, shock interaction heating levels between the intakes, and gap heating measurements under the fins.

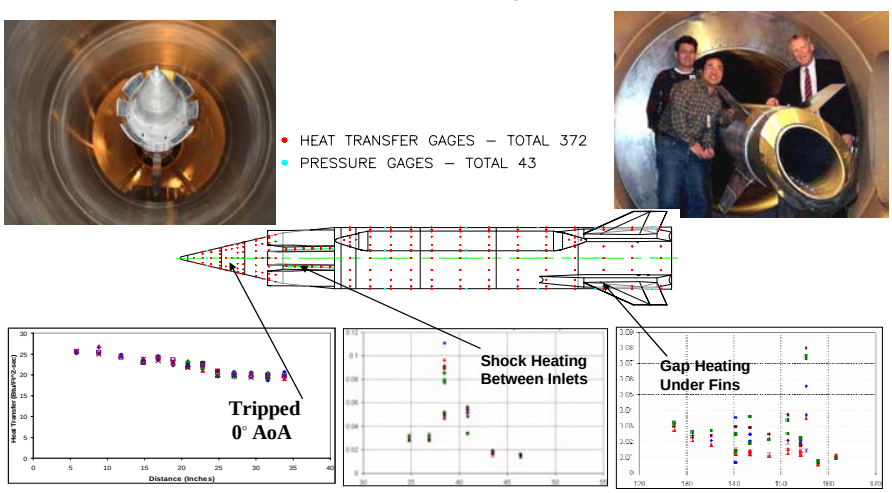

Figure 80: Full-Scale HyFly Aerothermal Studies in LENS II at Mach 6 Duplicated Flight Condition

Some of the most recent studies conducted in the LENS tunnels were to develop the HyCause “inward turning” engine for DARPA to be employed in flight tests conducted in the Australian HyShot series.

The basic vehicle configuration and a full-scale ground test model which was tested in LENS I and II are shown in Figure 81.

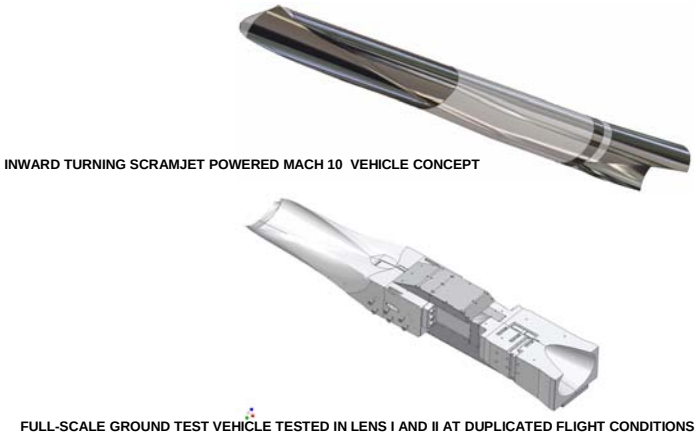

Figure 81: Full-Scale Studies of "Inward Turning" Engine

A significant effort was expended in the design and optimization of the inlet and the position and size of the trips to ensure that a turbulent flow entered the isolator. Pressure contours developed in the numerical simulations are shown in Figure 82. The trip configurations employed in the inlet are shown in Figure 83 together with the installation diagram for the HyCause engine in the LENS I facility.

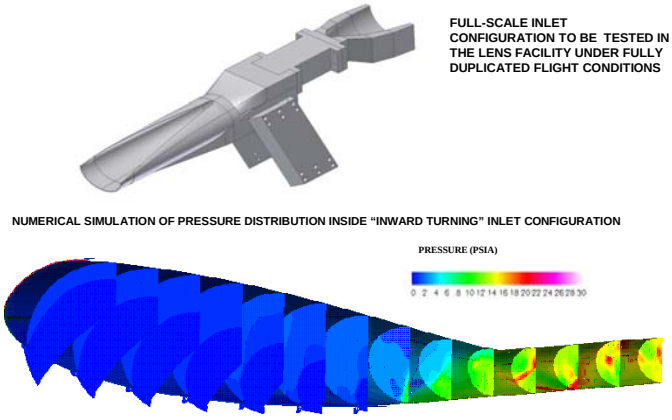

Figure 82: Experimental and Numerical Evaluation of "Inward Turning" Inlet Configurations

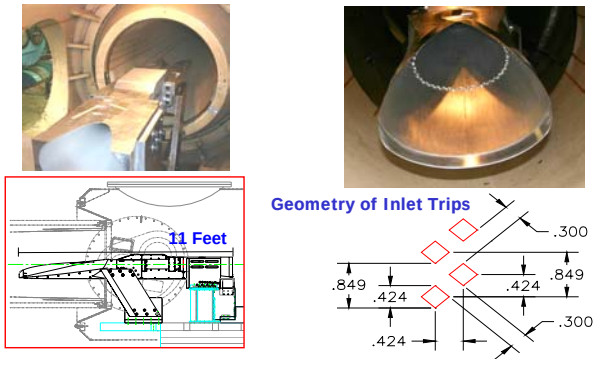

Figure 83: ITEC Installed in LENS I Tunnel

The HyCause model was highly instrumented with over 400 pressure and heat transfer gages as illustrated in Figure 84.

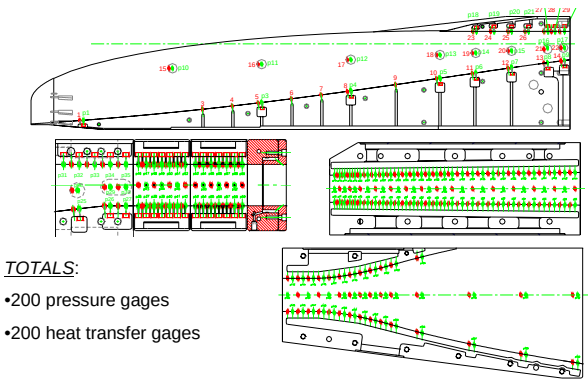

Figure 84: Engine Instrumentation

We also employed nonintrusive IR and laser diagnostics as well as pitot and total temperature probes to evaluate the flow through the engine as illustrated in Figure 85.

- Flowfield surveys using pitot and total temperature probes
- Infrared measurements to provide information on the existence position and extent of the region of combustion in the engine
- Laser Diode technique to measure the distribution of combustion products

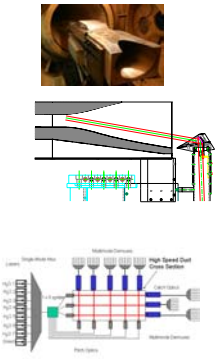

Figure 85: Flowfield Surveys at Exit of Combustor Made using Survey Rakes, Nonintrusive Infrared and Laser Diode Techniques

Typical intrusive and nonintrusive measurements made in these studies are shown in Figure 86 together with calculations made with Navier-Stokes prediction techniques.

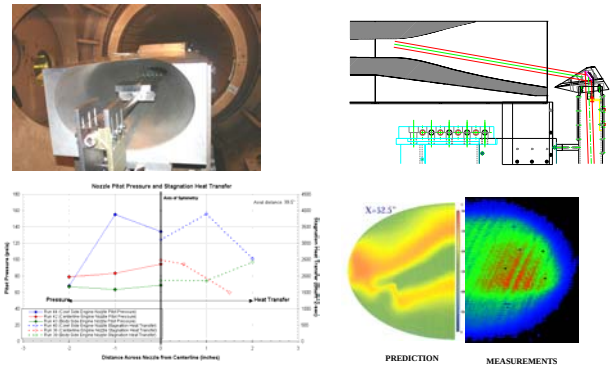

Figure 86: Survey Rake and Nonintrusive Infrared Measurements to Evaluate Combustor Performance

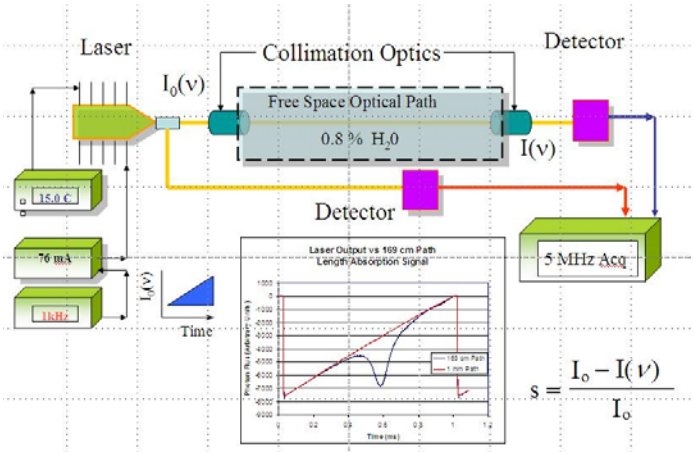

Figure 87: Schematic Diagram of Laser Diode System for Water Vapor and Temperature Measurements in Scramjet Engines

A schematic of the laser diode system employed to measure water vapor and temperature at the back of the engine and the hardware associated with the tomography system are shown in Figures 87 and 88. We are continuing to develop these systems and the results of these measurements are of key importance in optimizing the fuel injection systems and engine geometry.

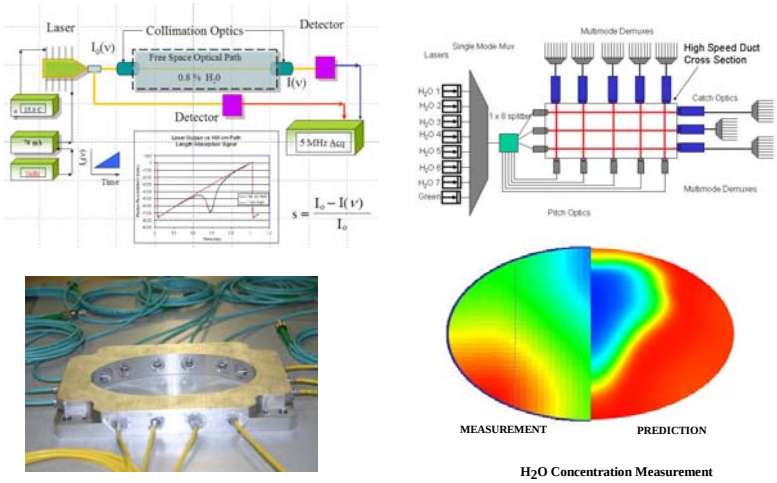

Figure 88: Water Vapor Measurements at End of HyCause Combustor with Laser Diode Tomography System

7.1 Studies to Develop Starting Mechanisms for Highly Contracted Inlet Systems

In order to start the HyCause engine, which was designed to have a significant internal contraction ratio, it is necessary to initiate the flow with a starting door open. The inlet modified to incorporate a starting door is shown in Figure 89. In these studies conducted in the LENS II facility with the full size scramjet engine, we also employed an isolator door (Figure 89) to ensure a stagnated flow through the engine during the initial part of the test series. Once flow was established over the engine, the isolator door was opened and then the bypass door was closed allowing the engine to successfully start as illustrated in Figures 89, 90 and 91.

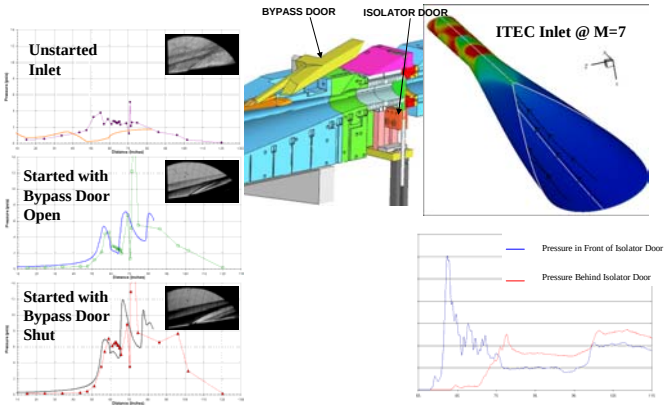

Figure 89: Test Time Requirements for Mode Switching and Scramjet Starting Studies (T_{test} = 70 ms)

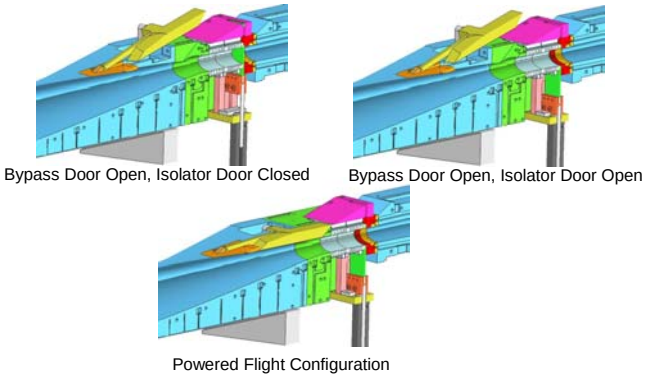

Figure 90: Engine Start Test Sequence

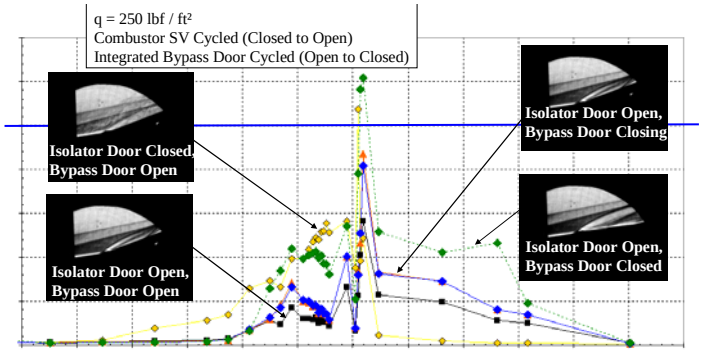

Figure 91: Flowfield and Pressure Distribution during Engine Start Process: Result: Bypass Door Enables Inlet/Engine to Start at High Altitude

8.0 STUDIES OF SHROUD, STORES AND STAGE SEPARATION

Many hypersonic missiles employ a shroud to cover the seekerhead or inlets of the vehicle during launch which is dispensed higher in the atmosphere. Ensuring that the dispensed shroud does not subsequently hit and damage the vehicle or influence the trajectory is of major concern to the designer. Also the trajectory of stores as they are dispensed from a hypersonic vehicle is of major concern for the same reason. Tests to evaluate the dynamic response of the shroud as it separates from the vehicle body can be conducted in wind tunnels. However, in high Mach number flow, the energy levels of the flying components can be extremely large.

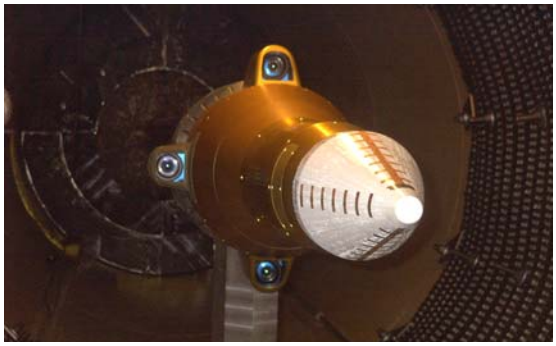

Figure 92: Tunnel Tests of Full-Scale Shroud Separation Model Prior to Flight Test Program

One way of minimizing the potential energy of the flying object is to stop the flow immediately as the shroud or munition is dispensed and this is done by a high speed valve. This is accomplished in the LENS II facility using a high speed valve which is timed to close when the shroud or other flying object has dispensed successfully. Figure 92 shows the tests which were conducted in the LENS II facility in which a full-scale two-part shroud was separated from the nosetip at duplicated flight conditions.

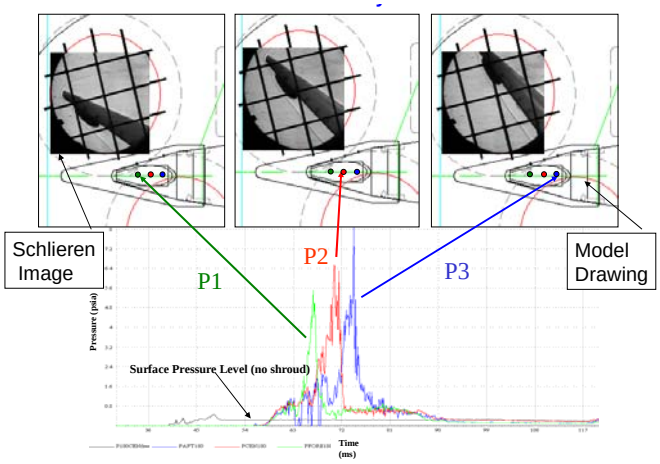

Figure 93: Shroud Separation Tests Demonstrating Large Unsteady Transient Loads Generated by Shock Interaction

Measurements were obtained with onboard cameras (shown in Figure 92) and with side mounted cameras which obtained the photographs in Figure 93. In addition to concerns on the trajectory of the shroud, the aero loads on the window beneath the shroud generated as the shock from the shroud

swept across the window were of major concern. As shown in Figure 93, pressure enhancement factors of over 30 were generated during this process.

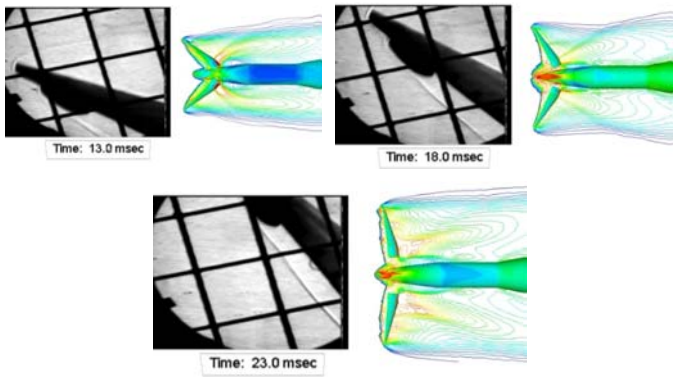

Figure 94: Comparison with Numerical Prediction

Figure 94 shows comparisons between the predictions a code employing unsteady Navier-Stokes equations and the tunnel results. Numerical predictions suffered from problems associated with accurately describing the shock/boundary layer interaction phenomena on the vehicle window and thus did not accurately reflect the experimental results.

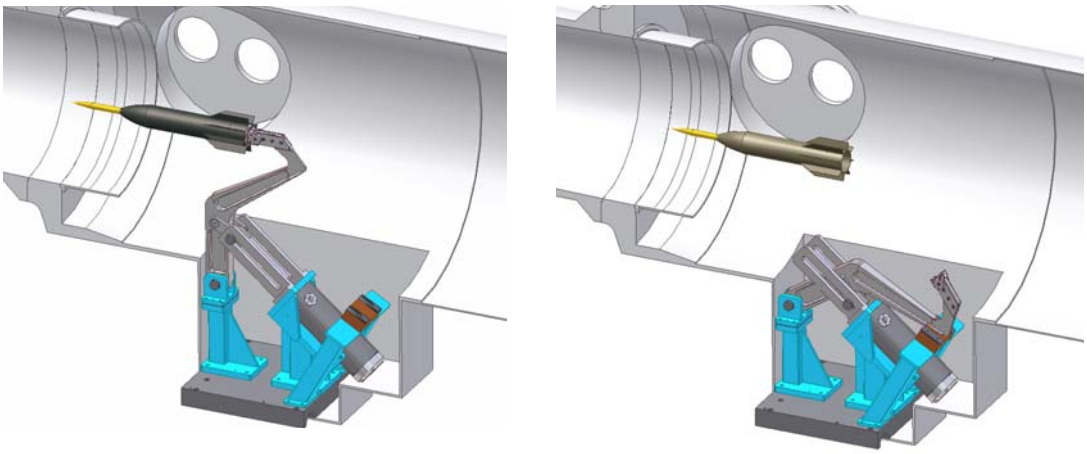

Figure 95: Diagram of Penetrator Weapon Systems deployed with the Rapid Retractable Support System (RRSS) in LENS II

Another major area for which ground tests can be employed to evaluate and validate vehicle design before it is committed to flight is in the area of stores and stage separation. Again employing fast-acting valve systems to stop the tunnel flow abruptly once the separation is achieved, a release system must be developed which can deploy the flying article without introducing extraneous motion. Figure 95 shows the launch system employed in the LENS II facility in studies to examine the separation of a two-stage launch system.

Here, the retractable support arm is activated in 4 ms just after flow is fully established over the two-stage vehicle. The vehicle is then free to "fly" and in this particular test, a launch vehicle is drag separated from the penetrator as illustrated in the high speed sequence of images taken during the LENS II test program (Figure 96).

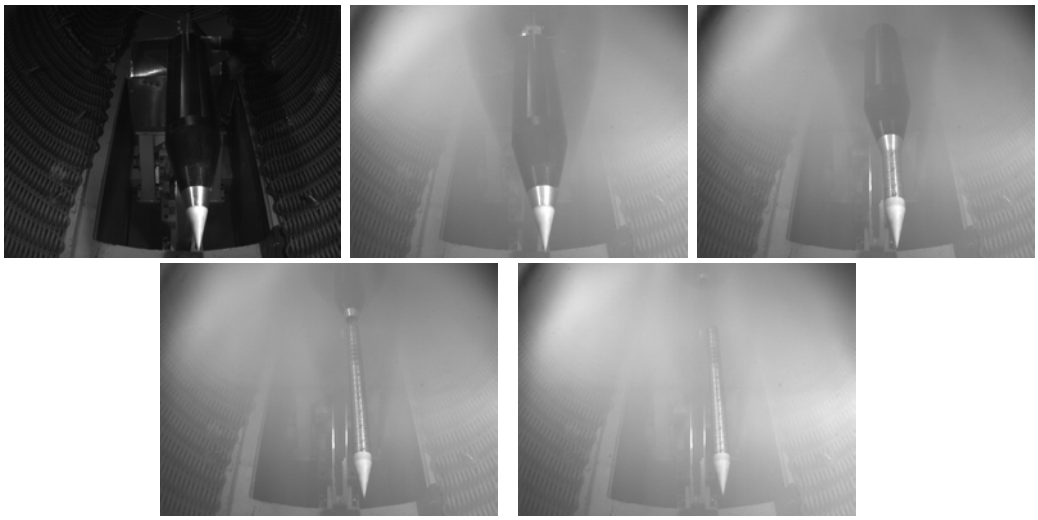

Figure 96: Sequence of High Speed Images taken during Penetrator/Booster Separation

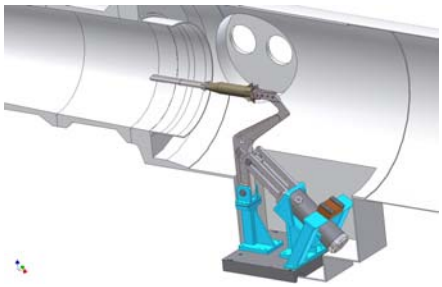

Figure 97: Quarter-Scale Scramjet Powered Vehicle Configuration for Launch with Rocket Booster

We are planning to employ this system to investigate the separation of a scramjet interceptor vehicle from the rocket system which boosts it to cruise velocity (as illustrated in Figure 97). A schematic representation of this process is shown in Figure 98.

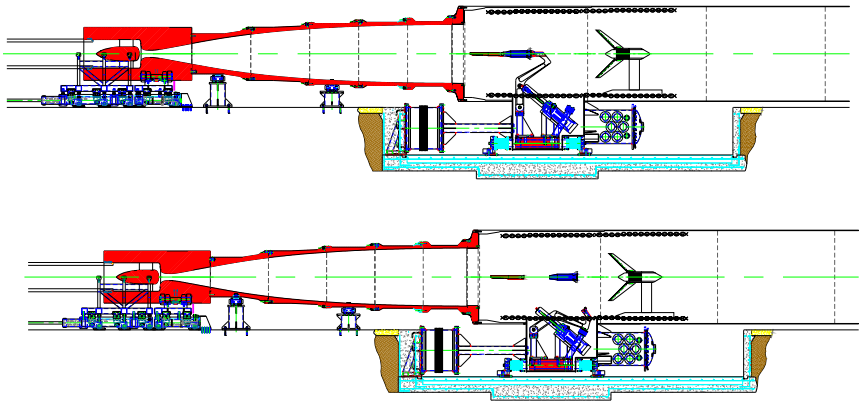

Figure 98: Studies of Stage Separation for Boost-to-Cruise Scramjet Powered Interceptor

9.0 MAJOR CONCLUSIONS

- Ground tests at fully duplicated or well simulated flight conditions are essential to minimize the risks associated with flight test programs from the perspective of overall vehicle performance and detailed measurements to investigate flow phenomena associated with real gas effects, boundary layer transition, turbulence and shock interaction phenomena and mixing and combustion
- Both flight test and ground test planning and evaluation should be totally integrated and supported by detailed numerical computations employing DSMC, Navier-Stokes and empirical prediction methods
- Hypersonic ground test facilities are available to perform full-scale testing at fully duplicated flight conditions of vehicles up to 3 to 6 meters in length.
- Flight test programs should be conducted in concert with and not at the expense of improving our ground test facilities and measurements techniques